Pergamon

Geochimica et Cosmochimica Acta, Vol. 67, No. 20, pp. 3971–3989, 2003

0016-7037/03 $30.00 + .00

doi:10.1016/S0016-7037(03)00234-5

The Sources of water in Martian meteorites: Clues from hydrogen isotopes

N. Z. Boctor,[1,*] C.M. O'D. Alexander,[2] J. Wang,[2] and E. Hauri[2]

[1]Geophysical Laboratory and Center for High Pressure Research, Carnegie Institution of Washington, 5251 Broad Branch Road, Washington, DC 20015, USA

[2]Dept. Terrestrial Magnetism, Carnegie Institution of Washington, 5241 Broad Branch Road, Washington, DC 20015, USA

(*Received May* 16, 2002; *accepted in revised form March* 31, 2003)

Abstract—H isotope measurements of carbonate, phosphate, feldspathic and mafic glasses, and post-stishovite silica phase in the shergottites Zagami, Shergotty, SaU 005, DaG 476, ALHA 77005 and EETA 79001, as well as in Chassigny and ALH 84001, show that all these phases contain deuterium-enriched water of extraterrestrial origin. The minerals and glasses analyzed may contain an initial primary hydrogen component, but their isotopic composition was modified to varying degrees by three different processes: interaction with a fractionated exchangeable water reservoir on Mars, hydrogen devolatilization by impact melting, and terrestrial contamination. Positive correlations between δD and water abundance in feldspathic glass and post-stishovite silica in Zagami, Shergotty, and SaU 005 is indicative of mixing of a high δD component (3000–4000‰) and a less abundant, low δD component (~0‰). The high δD component is primarily derived from the Martian exchangable reservoir, but may also have been influenced by isotopic fractionation associated with shock-induced hydrogen loss. The low δD component is either a terrestrial contaminant or a primary "magmatic" component. The negative correlation between δD and water abundances in mafic and feldspathic glasses in ALH 84001, ALHA 77005, and EETA 79001 is consistent with the addition of a low δD terrestrial contaminant to a less abundant high-deuterium Martian component. The low δD of magmatic glass in melt inclusions suggests that the δD of Martian parent magma was low and that the initial H isotope signature of Mars may be similar to that of Earth.

1. INTRODUCTION

The origin and behavior of water and other volatiles on Mars are fundamental to the understanding of the geological, geochemical, and climatological evolution of the planet. A tracer of perhaps the most important of these volatiles, water, is the isotopic composition of hydrogen. The hydrogen isotopic composition of the present-day Martian atmosphere is enriched in deuterium by a factor of 5.2 (δD = 4200 ‰) relative to mean terrestrial ocean water (Bjoraker et al., 1989), probably as the result of hydrogen escape to space (Owen et al., 1988; Bjoraker et al., 1989).

Leshin and co-workers (Watson et al., 1994; Leshin et al., 1996) reported large variations in the bulk δD values of several Martian meteorites (250–2100 ‰), as well as in individual minerals (512–4358 ‰). Based on these and other results, it has been suggested (Watson et al., 1994; Leshin et al., 1996; Jakosky and Jones, 1997) that at least two volatile reservoirs exist on Mars: a near-surface reservoir that is isotopically fractionated because it has undergone exchange with the atmosphere (hereafter, the exchangeable reservoir) and a deeper, unfractionated one that may represent a juvenile Martian reservoir. The isotopic composition of the Martian atmosphere, and, therefore, the reservoir(s) it exchanges with, is likely to have evolved with time. In principle, Martian meteorites with a range of ages could provide information on the δD evolution of the magmatic and exchangeable reservoirs on Mars.

For this investigation, we selected the following meteorites: ALH 84001, a Martian orthopyroxenite; the shergottites EETA 79001, ALHA 77005, Zagami, Shergotty, Dar al Gani (DaG 476), and Sayh al Uhaymir (SaU 005); and the Martian dunite Chassigny. These meteorites range in age from 4.5 Gyr to 130 million years, and display different degrees of shock metamorphism. We have determined the hydrogen isotopic compositions and water contents of mineral phases and glasses in these meteorites by secondary ion mass spectrometry (SIMS). The H isotope data are used in conjunction with the petrology and shock metamorphic effects to assess the source and history of water in these Martian meteorites.

2. TECHNIQUES

The petrography of these meteorites was studied in both reflected and transmitted light, and the shock metamorphic effects were documented in detail. Shock pressures were estimated from the data of Stöffler et al. (1991), Bischoff and Stöffler (1992) and Schaal and Hörz (1977). The compositions of the phases to be analyzed by ion microprobe were determined by electron microprobe. The analyses were performed with a Jeol superprobe at 15 kV and typically with a 20 nA beam. To avoid vaporization of the alkali elements when analyzing feldspathic glass, silica phases, and melt inclusion glasses, the beam current was reduced to 5 nA and, if the size of the grain allowed, the beam was rastered over an area of 10×10 μm. The standards used are synthetic pyroxene, orthoclase, apatite, and diopside doped with minor amounts of Ti, Mn, and Cr.

SIMS measurements were made with a Cameca 6f ion microprobe. The experimental procedure for trace element measurements are similar to the approach of Zinner and Crozaz (1986). Measurements were made at a mass resolution of ~400 with a 12.5 kV O^- primary ion beam, a 10 kV secondary

* Author to whom correspondence should be addressed (boctor@gl.ciw.edu).

accelerating voltage with a 75 V offset, and a 50 eV energy window. The elemental concentrations were determined relative to Si for silicates, and Ca for phosphates and carbonates. The SiO_2 and CaO contents of the samples were previously determined by electron microprobe. Corrections for isobaric interferences were made following the procedures of Zinner and Crozaz (1986) and Alexander (1994). Sensitivity factors relative to Si and Ca were determined using NBS-610 and NBS-612 glasses.

Operating conditions for H and O isotope measurements were: 15 kV Cs^+ primary beam of ~2 nA, −5 kV secondary accelerating voltage, a 50 eV energy window, a mass resolution of ~400, an electron flood gun for charge compensation, and, in most cases, a 100 μm field aperture. When using a Cs^+ primary beam, the H_2/D ratio is typically <0.0015 (Hauri et al., 2002), so it is not necessary to resolve H_2 from D. For the $\delta^{18}O$ isotope measurements, a 350 V offset was used to reduce isobaric interferences (Hervig and Steele, 1992), with a flat bottomed primary beam ~20–25 μm across. Only the measurements of phosphates are reported here, for which Jacupiranga apatite (Santos and Clayton, 1995) was used to determine the instrumental mass fractionation.

For the H isotope measurements, the analyzed areas ranged between 5 μm and 25 μm across. A few analyses were made with an O^- primary beam with a 10 kV secondary accelerating voltage and a mass resolution of ~1500. The results were comparable to those made with the Cs^+ beam. More detailed discussions of techniques for H isotope and abundance measurements can be found in Hauri et al. (2002) and Koga et al. (2003). Hauri et al. (2002) showed that the magnitudes of matrix effects in the Cs-based method for measuring D/H ratios are reduced by a factor of two compared to those of the O method. For example, the total range in D/H matrix effects is only 50 ‰ in rhyolite glasses that range from 0.1 to 5 wt.% H_2O and is even smaller in basalts and amphiboles. The analytical errors in our Martian δD measurements are in most cases >50 ‰. Therefore, the matrix effects are not significant at the level of precision of the δD values reported here.

The H isotope instrumental mass fractionation, and the H/Si and H/O sensitivity factors for water abundance measurements, were determined using three rhyolite glasses (MC84-t, NW Coulee and Panum Dome; Newman et al. (1988)) and two amphiboles (Bamble and Beta Hochee; Deloule et al. (1991)) for silicates, and Jacupiranga apatite (Nadeau et al., 1999) for phosphates. There are no systematic difference in the instrumental mass fractionation between the rhyolite glasses and the amphiboles.

Water abundances determined using the H/Si and H/O sensitivity factors were typically within 10–20% of one another. However, there does seem to be slight differences in the H/Si sensitivity factors determined with the rhyolite glasses and the amphiboles. The most analyzed amphibole and rhyolite glass were respectively Bamble (2.03 wt.% water, 51.48 wt.% SiO_2, 44.3 wt.% O) and MC84-t (0.78 wt.% water, 76.63 wt.% SiO_2, 49.58 wt.% O). For our entire set of runs, the means and standard deviations of the ratios (Bamble/MC84-t) of the Si and O sensitivity factors determined from them were 1.50 ± 0.15 and 1.02 ± 0.12, respectively. The Si sensitivity factor is apparently more matrix sensitive than the O sensitivity factor. Therefore, the water abundances calculated using the H/O sensitivities were used for silicates. The H/O sensitivity factors for silicates and phosphates are within 30% of one another. We were unable to obtain carbonate standards and used a mean of the silicate and phosphate H/O sensitivity factors. The water contents in the ALH 84001 carbonates appear to be quite high. We cannot rule out that this reflects a large difference in the H/O sensitivity factors between silicates/phosphates and carbonates.

Hydrogen contamination of sections during preparation, storage and during measurements is a significant problem. Water and hydrocarbons from the air and the vacuum system are adsorbed onto the surfaces. To minimize these sources of contamination, all samples/standards were kept for at least 1.5–2 days in the pump down chamber of the instrument at high vacuum ($<10^{-8}$ torr) while being warmed (<70°C) under a heat lamp. The samples were also sputtered for 5 min before the start of an analysis.

To test for possible contamination by epoxy in silicates and phosphates, and silicate contamination of phosphates and carbonates, ^{12}C and ^{30}Si were measured in most cases. Estimates of the maximum contamination from epoxy ($H^-/^{12}C^- = 0.015$) in non-carbonate phases assuming all C counts were from epoxy were always small (≤60‰). Variations in the D^-/H^-, and $^{12}C^-/H^-$ and $^{30}Si^-/H^-$ ratios during an analysis were common. Only those portions of an analysis when the above ratios had reached essentially constant values, typically towards the end of an analysis, were used. Also, only silicate analyses with low $^{12}C^-/H^-$ and $^{12}C^-/^{30}Si^-$ ratios, carbonates with low $^{30}Si^-/H^-$ and $^{30}Si^-/^{12}C^-$ ratios and phosphates with low $^{30}Si^-/H^-$ and $^{12}C^-/H^-$ ratios were used.

Perhaps more difficult contaminants to eliminate are oils and/or water used as lubricants during section preparation, and water, methanol, acetone etc. that are used for cleaning. These contaminants may be able to interact with or diffuse into samples, particularly if the samples have microfractures as most shocked materials are likely to have. Finally, we have found that carbon coats generally contribute significantly to the hydrogen blank. When possible we have removed the carbon coat by polishing and recoated the sample with gold. However, it is not always possible to remove all of the coat from highly fractured areas.

3. PETROGRAPHY AND MINERAL CHEMISTRY

3.1. Allan Hill 84001 (ALH 84001)

The petrography of ALH 84001 was described by Mittlefehldt (1994), Treiman (1995), and Greenwood and McSween (2001). ALH 84001 is a coarse-grained cataclastic orthopyroxenite composed mainly of orthopyroxene ($Mg_{70}Fe_{26}Ca_4$) with clinopyroxene ($Mg_{42}Fe_{14}Ca_{44}$), feldspathic glass, chromite, phosphate minerals, and carbonate as minor phases. Shock features in ALH 84001 are represented by fracturing and deformation in orthopyroxene and transformation of the feldspar to glass by shock melting at a pressure of ~40 GPa (400 kbars).

A unique feature in this meteorite is the occurrence of carbonates in impact generated cataclastic zones in orthopyroxene. The carbonates occur either as globules, displaying complex zoning, or as fine disseminated grains. The globules

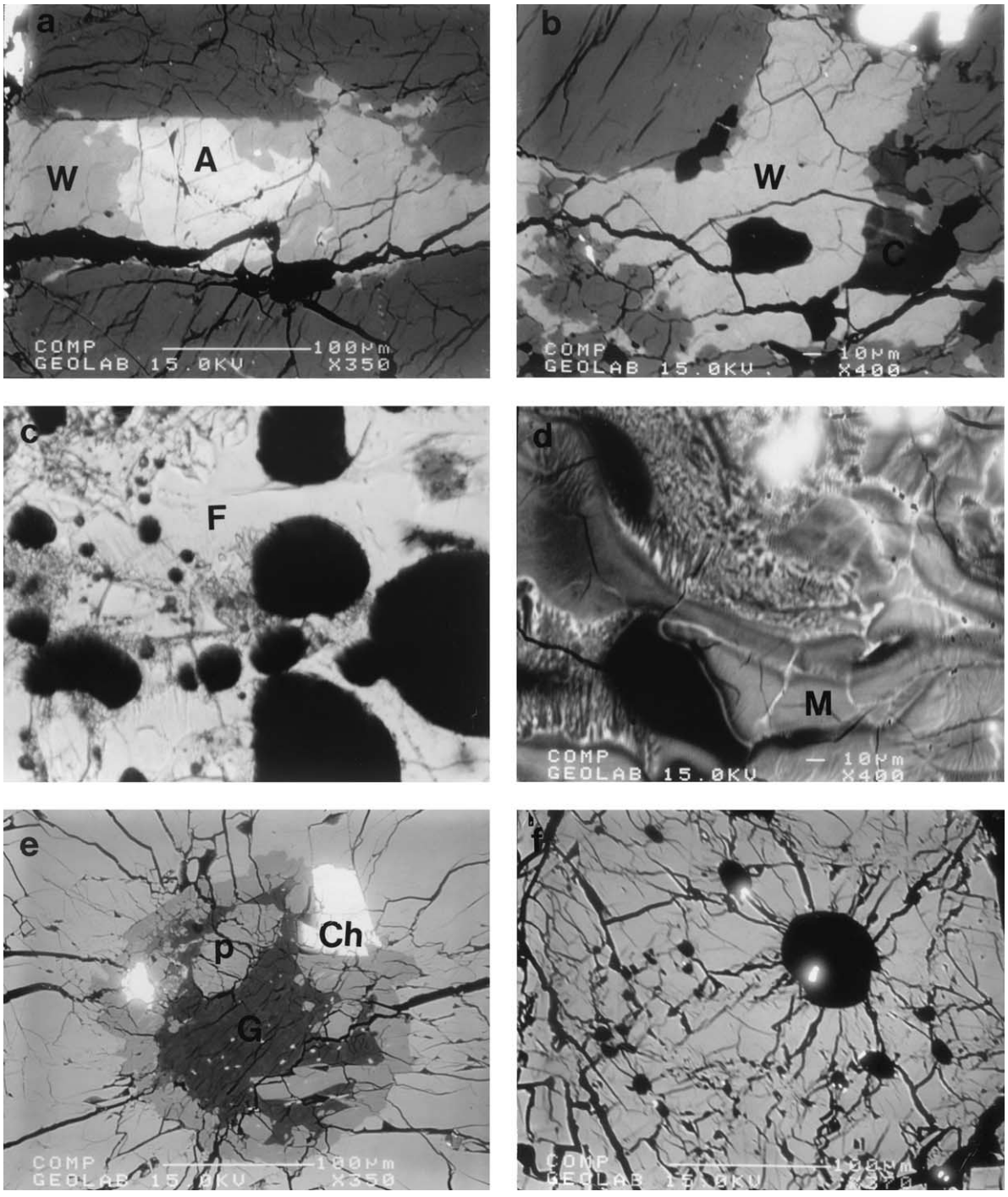

Fig. 1. (a) Apatite (A) mantled by whitlockite (W) in ALH 84001 (whitlockite grain 2 in Tables 1 and 2). (b) Whitlockite (W) showing zoned carbonate inclusions (nearly black) in ALH 84001 (whitlockite grain 3 in Table 2). (c) Feldspathic glass (F) with numerous vesicles (dark regions) in ALHA 77005. (d) Mafic glass (M) showing a flow structure in EETA 79001 with unmelted fragments enclosed in the glass. (e) Melt inclusion in Chassigny olivine, showing pyroxene crystals (P), chromite (Ch) and residual magmatic glass (G). (f) Highly fractured olivine with small glassy melt inclusions (black) in Chassigny. The largest inclusion at the center contains a crystal of pyrrhotite (white).

we analyzed were hemispherical, and none of them were perfect rosettes.

Three phosphate grains were found in two different polished thin sections. One phosphate grain (~400μm) was zoned with a chlorapatite core (~125μm, Cl=2.98–3.72 wt. %) and an annular whitlockite rim (whitlockite 2) (Fig. 1a, Table 1). The whitlockite rim contained traces of Cl and no detectable F. The other two grains (~800–1000μm) contained carbonate inclusions. In one of the grains (whitlockite 3), very magnesite-rich, occasionally zoned ($Mg_{0.952}Ca_{0.004}Fe_{0.007}$ to $Mg_{0.517}Ca_{0.145}$

Table 1. Representative electron microprobe analyses (wt. %) of whitlockite and apatite from ALH 84001.

	Whitlockite 2		
	Apatite Core	Whitlockite Rim	Whitlockite 1
Na_2O	0.34	2.57	2.46
MgO	0.02	3.43	3.48
CaO	53.82	47.11	46.43
FeO	0.15	0.83	0.58
SiO_2	0.22	0.04	0.07
Al_2O_3	n.d.	n.d.	n.d.
P_2O_5	41.20	44.98	46.64
F	1.29	n.d.	n.d.
Cl	3.42	n.d.	n.d.
Total	99.14	99.00	99.73

n.d. = not determined

$Fe_{0.339}$) carbonate occurs at its margins and as euhedral or subhedral inclusions (Fig. 1b). The other whitlockite grain (whitlockite 1) contained unzoned carbonates and is itself composed of numerous interlocking subgrains, perhaps due to shock induced recrystallization. Whitlockite 1 shows discontinuous thin rims of clinopyroxene ($En_{45}Fs_{13}Wo_{42}$) at its peripheries. In the regions of the grain where clinopyroxene is absent, whitlockite is in contact with orthopyroxene ($En_{71}Fs_{26}Wo_3$). Hydrogen isotope compositions and water abundances were determined for the carbonates, whitlockite, apatite, and feldspathic glasses (Table 2, Fig. 2).

3.2. Elephant Moraine 79001 (EETA 79001)

EETA 79001, a shergottite, consists of two basaltic lithologies (A and B) joined along a diffuse planar contact (Steele and Smith, 1982; McSween and Jarosewich, 1983; Mittlefehldt et al., 1999). A third lithology (C) of impact-produced glasses occurs as discontinuous pockets at the interfaces of lithologies A and B.

Lithology A is composed of a heterogeneous suite of olivine and orthopyroxene megacrysts with minor chromite in a matrix of devitrified basaltic glass. Boctor et al. (1998a, 1998b) noted that some olivine megacrysts are now composed of aggregates of two distinct α olivine compositions differing by ~30 mol % Fo. They attributed the compositional differences to the transformation of the olivine to a mixture of the α olivine and γ spinel structures during impact, with the γ phase inverting to the α olivine during the thermal annealing after decompression. The dynamic pressure range for the mixed phase region in the olivine phase diagram at high pressure is between 25 and 70 GPa. Boctor et al. (1998a, 1998b) noted that other olivine megacrysts are now composed of aggregates of spherules which they interpreted as devitrified diaplectic olivine glass produced by impact at ~55 GPa. Mittlefehldt et al. (1997, 1999) independently concluded on the basis of mixing models using major and trace elements that lithology A is an impact melt composed dominantly of basalt-like lithology B and lherzolitic cumulates. Thus, it is similar to the trace-element-poor fractions of ALHA 77005 and Y-793605.

Lithology B is a coarse-grained basalt. The olivine and pyroxene show fracturing and deformation, whereas the plagioclase completely transformed to feldspathic glass at shock pressures of ~40 GPa.

Table 2. The H isotopic compositions and water abundances of phases in ALH 84001.

Sample	δD (‰)	H_2O (ppm)
Feldspathic Glasses		
84001-FG-1	1234 ± 48	1090 ± 250
84001-FG-2	1620 ± 43	905 ± 120
84001-FG-3	1738 ± 36	760 ± 130
84001-FG-4	1074 ± 16	7200 ± 1100
84001-FG-5	1152 ± 28	1170 ± 230
84001-FG-6	1174 ± 20	2160 ± 760
84001-FG-7	1667 ± 41	1090 ± 120
84001-FG-8	1195 ± 20	1580 ± 200
84001-FG-9a	1591 ± 16	1810 ± 300
84001-FG-9b	1328 ± 23	2250 ± 660
84001-FG-10	1334 ± 47	1380 ± 280
84001-FG-11	1116 ± 30	316 ± 77
Phosphates		
Whitlockite		
84001-WT-1	406 ± 28	1690 ± 300
84001-WT-2a	135 ± 36	900 ± 140
84001-WT-2b	297 ± 20	1200 ± 380
84001-WT-2c	156 ± 17	n.m.
84001-WT-3a	148 ± 7	1700 ± 370
84001-WT-3b	103 ± 14	1080 ± 180
84001-WT-3c	144 ± 16	1200 ± 130
84001-WT-3d	113 ± 49	920 ± 90
84001-WT-3e	92 ± 34	2110 ± 190
Apatite		
84001-AP-1[a]	751 ± 19	2210 ± 290
Carbonates		
84001-CW-1[b]	1045 ± 22	3640 ± 490
Globules		
84001-CG-1a	1196 ± 47	7330 ± 680
84001-CG-1b	821 ± 22	8000 ± 790
84001-CG-2	781 ± 30	9860 ± 850
84001-CG-3	331 ± 12	11000 ± 1000
84001-CG-4a	412 ± 14	8700 ± 2200
84001-CG-4b	1068 ± 22	4070 ± 350
Irregular grains[c]		
84001-CI-1a	839 ± 12	9440 ± 900
84001-CI-1b	427 ± 19	6040 ± 560
84001-CI-2a	1004 ± 16	7000 ± 680
84001-CI-2b	481 ± 13	11400 ± 1100

[a] This apatite was surrounded by whitlockite grain 2 (see Table 1 and Fig. 1).
[b] This carbonate was an inclusion in whitlockite grain 3.
[c] These grains were located in crushed zones. n.m. = not measured.

Lithology C is composed entirely of glass. The mafic glass shows a flow structure (Fig. 1d) and occasionally incipient devitrification. The feldspathic glass in lithology C is commonly vesicular. Shock pressure for melting and vesiculation of the plagioclase is ≥45 GPa. The localized shock pressure that produced the mafic glass in lithology C and the impact melt of lithology A is 60–80 GPa. Hydrogen isotope and water abundance measurements were made for feldspathic glasses in lithologies B and C, and for mafic glasses in lithology C (Table 3, Fig. 5).

3.3. Allan Hill 77005 (ALHA 77005)

The petrography of ALHA 77005 was described by McSween et al. (1979), Treiman et al. (1994), and Mittlefehldt and

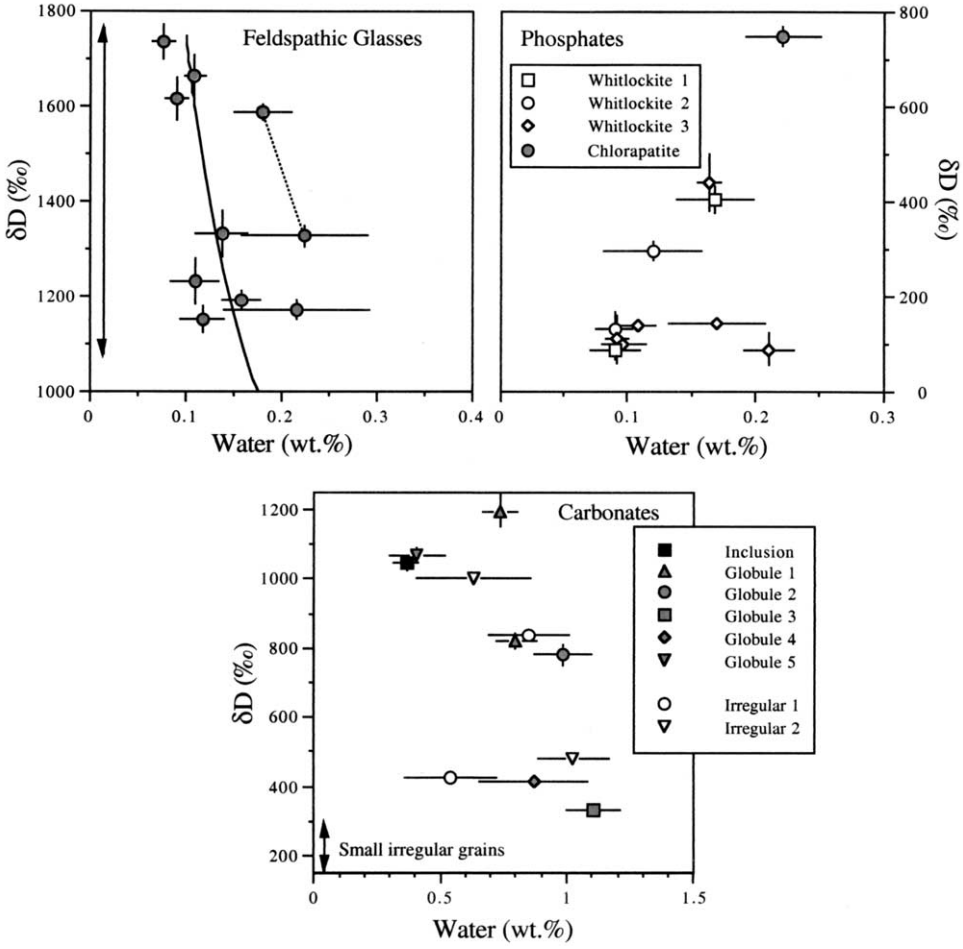

Fig. 2. The hydrogen isotopic compositions and water abundances in water-bearing phases of ALH 84001. The arrowed lines give the range of δD values for grains whose water abundances were not measured. In Figure 3b, two analyses of a single feldspathic glass grain are joined by a dashed line. Also shown is a mixing line in which an isotopically normal component (δD≈0‰) is being added to an isotopically anomalous component (δD=1750‰, H_2O≈1000 ppm). In Figure 3c, the carbonate inclusion was in whitlockite 1.

Lindstrom (1999). The meteorite is composed of olivine (Fo_{75-78}), pigeonite ($Mg_{68}Fe_{24}Ca_8$), augite ($Mg_{49}Fe_{17}Ca_{34}$), feldspathic glass, chromite, and ilmenite. Fine-grained whitlockite, apatite and pyrrhotite with pentlandite exsolutions are accessory phases. Shock metamorphic effects (Treiman et al., 1994; Boctor et al., 1999) are represented by fracturing and planar deformation features in olivine, deformation lamellae in pyroxene, and transformation of the plagioclase to feldspathic glass, which is occasionally vesicular (shock pressure ≥45 GPa) (Fig. 1c). Localized shock melting occurred and pockets of the melt show a spinifex texture. The olivine in the melt pockets is more magnesian than the original olivine (Fo_{86-81} vs. Fo_{71-65}). A similar trend is observed in pigeonite ($Mg_{64}Fe_{22}Ca_9$ vs. $Mg_{57}Fe_{35}Ca_8$). Residual glass occurs interstitially between the olivine crystals. Melt veins are common and consist of zoned olivine and skeletal pyroxene and residual glass. The shock pressure that caused the localized melting in ALHA 77005 ≥60 GPa.

Olivine in ALHA 77005 contains igneous melt inclusions composed of Al-rich, low-Ca pyroxene, feldspathic glass, and a silica-rich glass (95 wt.% SiO_2). Some inclusions show large tabular crystals of low-Ca pyroxene with interstitial rhyolitic glass (64–68 wt.% SiO_2). Hydrogen isotopes and water abundances were measured in the feldspathic glasses, in the mafic glass in one of the melt pockets, in a partially devitrified mafic glass in a melt vein, and in magmatic glasses in five melt inclusions (Table 4, Fig. 6).

3.4. Shergotty

The petrography and minor and trace element distributions were studied by Stolper and McSween (1979), Stöffler et al. (1986), and Wadhwa et al. (1994). Shergotty is composed of cumulate pigeonite (core $Ca_{34}Mg_{48}Fe_{18}$, rim $Ca_{32}Mg_{44}Fe_{23}$) and augite (core $Ca_{12}Mg_{61}Fe_{27}$, rim $Ca_{15}Mg_{50}Fe_{35}$) with interstitial plagioclase that was transformed by impact melting to feldspathic glass.

Silica is an accessory mineral in Shergotty and occurs either as a discrete phase showing a lamellar structure or as a silica-feldspathic glass intergrowth. The silica in the intergrowths is optically isotropic and, therefore, probably a glass. The discrete silica was found by Sharp and El Goresy (1999) to be a high pressure polymorph of silica, which shows evidence of partial

Table 3. The H isotopic compositions and water abundances of phases in EETA 79001.

Sample	Lithology	δD (‰)	H_2O (ppm)
Mafic glasses			
79001-MG-1	C	2670 ± 100	295 ± 27
79001-MG-2	C	2782 ± 37	259 ± 22
79001-MG-3	C	2590 ± 120	334 ± 32
79001-MG-4	C	2748 ± 97	556 ± 70
79001-MG-5	C	2900 ± 16	180 ± 40
79001-MG-6	C	2289 ± 53	534 ± 58
79001-MG-7	C	2740 ± 40	270 ± 27
79001-MG-8	C	1697 ± 43	209 ± 34
Feldspathic glasses[a]			
79001-FG-1	C	1709 ± 78	142 ± 14
79001-FG-2	B	1540 ± 100	128 ± 11
79001-FG-3	B	1589 ± 67	111 ± 17
79001-FG-4	C	2753 ± 41	101 ± 15
79001-FG-5	C	2087 ± 49	74 ± 7
79001-FG-6	C	1717 ± 61	108 ± 12
Olivine			
79001-OL-1	B	1303 ± 66	29 ± 3
Orthopyroxene			
79001-PX-1	B	−26 ± 13	92 ± 9
Apatite[b]			
79001-AP-1	B	146 ± 25	1160 ± 100

[a] The feldspathic glasses are from lithology C and are typically vesicular.
[b] This was a needle shaped grain, so the analysis may have sampled surrounding silicates.

Table 4. The H isotopic compositions and water abundances of phases in ALHA 77005.

Sample	δD (‰)	H_2O (ppm)
Mafic glasses		
77005-MG-1[a]	3030 ± 130	520 ± 150
77005-MG-2[b]	1301 ± 74	105 ± 12
Feldspathic glasses		
77005-FG-1[c]	2536 ± 89	98 ± 10
77005-FG-2	2370 ± 73	86 ± 9
77005-FG-3	2170 ± 120	91 ± 9
77005-FG-4	1820 ± 140	147 ± 26
77005-FG-5[c]	4021 ± 68	95 ± 11
77005-FG-6	2266 ± 53	388 ± 43
77005-FG-7	1892 ± 63	126 ± 14
77005-FG-8[c]	4091 ± 77	61 ± 7
77005-FG-9[c]	3785 ± 47	178 ± 20
77005-FG-10	982 ± 24	930 ± 100
77005-FG-11	4214 ± 67	80 ± 9
77005-FG-12	3245 ± 67	74 ± 8
Melt Inclusions		
77005-IN-1	304 ± 67	1.1 ± 0.2
77005-IN-2	293 ± 80	1.2 ± 0.3
77005-IN-3	−18 ± 25	0.74 ± 0.13
77005-IN-4	−8 ± 23	357 ± 41
77005-IN-5	−106 ± 15	1770 ± 200
Olivine		
77005-OL-1	35 ± 280	0.53 ± 0.12
Whitlockite		
77005-WT-1	22 ± 15	6740 ± 750
Pigeonite		
77005-PX-1	69 ± 36	360 ± 110

[a] Glass in a shock melt pocket.
[b] Glass in a partially devitrified shock melt vein.
[c] Glass is vesicular.

amorphization during decompression. The structure of the high pressure silica phase is now recognized as the αPbO_2 structure (Dubrovinsky et al., 1997; Dera et al., 2002). It is often referred to as post-stishovite silica and in Shergotty is typically >98 wt.% SiO_2; the main impurities are Al_2O_3 (0.8 to 1.6 wt.%) and Na_2O (0.2 to 0.5 wt.%). Post-stishovite silica has been synthesized by Dubrovinsky et al. (2001) at 82 GPa and 950°K from cristobalite in a diamond anvil cell and at 45 GPa at room temperature from tridymite. The phases analyzed for H isotopes and water abundances in Shergotty were feldspathic glasses, post-stishovite silica, and silica-feldspathic glass intergrowths (Table 5, Fig. 7).

3.5. Zagami

Zagami was previously studied by, for example, McCoy et al. (1992), Treiman and Sutton (1992), and Wadhwa et al. (1994). Like Shergotty, Zagami is composed of cumulate augite and pigeonite, with tabular or anhedral plagioclase transformed to nonvesicular glass. Silica (probably glass) intergrown with a phase of feldspathic composition is more common in Zagami than in Shergotty. Two types of this intergrowth are found: a fine mermykitic intergrowth and a more coarse-grained symplectite. Boctor et al. (2001) also reported the presence of post-stishovite silica (αPbO_2 structure) in Zagami. The phases analyzed are feldspathic glasses, post-stishovite silica, and the symplectite of silica and feldspathic glass (Table 6, Fig. 8).

3.6. Dar al Gani (DaG 476)

The petrology and minor and trace element distributions in this meteorite have been investigated by Zipfel et al. (2000), Wadhwa et al. (2001), and Mikouchi et al. (2001). DaG 476 is composed mainly of low-Ca pyroxene ($Mg_{74}Fe_{22}Ca_4$ to $En_{57}Fe_{31}Ca_{10}$) and olivine (Fo_{74-60}) with interstitial feldspathic glass. Whitlockite and secondary terrestrial carbonates are present as minor constituents. The olivine was interpreted by Mikouchi et al. (2001) as xenocrystic, although Zipfel et al. (2000) believe that the euhedral to subhedral olivine are phenocrysts that crystallized directly from the magma. Both olivine and pyroxene show mineral zoning with the cores being enriched in Mg relative to the rims. DaG 476 is believed to have crystallized from a more primitive mafic magma than lithology A in EETA 79001, and it may have an impact melt origin (Mikouchi et al., 2001). The phase analyzed in Dar al Gani is impact-melted feldspathic glass (Table 7, Fig. 9).

3.7. Sayh al Uhaymir (SaU 005)

A brief petrographic description of the Saharan meteorite SaU 005 was given was given by Zipfel et al. (2000). SaU 005 shows some similarities to DaG 476. It contains olivine megacrysts (Fo_{70-64}) in a more fine-grained groundmass of pigeonite ($Mg_{80}Fe_{13}Ca_7$ — $Mg_{59}Fe_{26}Ca_{15}$) and feldspathic glass. SaU 005, like DaG 476, shows chemical and mineralogical affinities to the lherzolitic shergottites. Shock metamorphic effects in SaU 005 are similar to those observed in EETA 79001 and ALHA 77005. Quenched melt pockets show a spinifex texture, like in ALHA 77005. As in EETA 79001, some olivine megacrysts transformed to a mixture of the α and

Table 5. The H isotopic compositions and water abundances of phases in Shergotty.

Sample	δD (‰)	H_2O (ppm)
Feldspathic Glasses		
SHRG-FG-1	1577 ± 64	89 ± 6
SHRG-FG-2a	669 ± 67	50 ± 4
SHRG-FG-2b	646 ± 71	50 ± 4
SHRG-FG-3	398 ± 67	54 ± 4
SHRG-FG-4	1394 ± 79	63 ± 4
SHRG-FG-5	701 ± 82	72 ± 5
SHRG-FG-6	688 ± 34	41 ± 4
SHRG-FG-7	877 ± 34	57 ± 6
SHRG-FG-8	−15 ± 56	44 ± 3
SHRG-FG-9	−9 ± 57	50 ± 4
SHRG-FG-10a	−84 ± 55	47 ± 3
SHRG-FG-10b	−83 ± 53	57 ± 4
SHRG-FG-11	−106 ± 67	46 ± 3
SHRG-FG-12	97 ± 24	57 ± 6
SHRG-FG-13	80 ± 39	49 ± 5
SHRG-FG-14	−79 ± 36	29 ± 3
Silica		
SHRG-SI-1	1793 ± 61	267 ± 19
SHRG-SI-2	1975 ± 27	239 ± 25
SHRG-SI-3	1246 ± 38	179 ± 19
Silica-Plagioclase Intergrowths		
SHRG-SP-1	441 ± 17	662 ± 69
SHRG-SP-2	490 ± 23	111 ± 12
Pigeonite		
SHRG-PX-1	−60 ± 49	800 ± 56
SHRG-PX-2	−153 ± 23	1360 ± 140

γ polymorphs by impact; the γ phase later transformed to the α structure, and the megacrysts are now composed of aggregates

Table 6. The H isotopic compositions and water abundances of phases in Zagami.

Sample	δD (‰)	H_2O (ppm)
Feldspathic Glasses		
ZAG-FG-1	1243 ± 73	55 ± 4
ZAG-FG-2	1886 ± 63	90 ± 6
ZAG-FG-3	2214 ± 51	59 ± 7
ZAG-FG-4	1645 ± 37	32 ± 4
ZAG-FG-5	687 ± 36	22 ± 2
ZAG-FG-6	945 ± 51	21 ± 2
ZAG-FG-7	2282 ± 40	45 ± 5
ZAG-FG-8	1311 ± 46	31 ± 3
ZAG-FG-9	617 ± 52	16 ± 2
ZAG-FG-10	1156 ± 48	18 ± 2
ZAG-FG-11	579 ± 47	11 ± 1
ZAG-FG-12	1101 ± 67	12 ± 1
ZAG-FG-13	1571 ± 47	20 ± 2
Silica		
ZAG-SI-1	2303 ± 53	56 ± 6
ZAG-SI-2	2704 ± 47	61 ± 7
ZAG-SI-3	1760 ± 35	183 ± 20
ZAG-SI-4	1173 ± 77	30 ± 3
Silica-Plagioclase Intergrowths		
ZAG-SP-1	1195 ± 36	338 ± 38
ZAG-SP-2	285 ± 26	496 ± 56
ZAG-SP-3	636 ± 32	576 ± 69
ZAG-SP-4	577 ± 23	624 ± 69
Pigeonite		
ZAG-PX-1	−204 ± 5	3360 ± 370

Table 7. The H isotopic compositions and water abundances of shock produced feldspathic glasses from the meteorites SaU 005 and DaG 476.

Sample	δD (‰)	H_2O (ppm)
SAU 005		
SAU-FG-1	−105 ± 17	1900 ± 210
SAU-FG-2	3260 ± 40	17400 ± 1900
SAU-FG-3	−52 ± 16	76200 ± 8400
SAU-FG-4	−31 ± 16	18000 ± 2000
SAU-FG-5	743 ± 31	177 ± 20
SAU-FG-6	974 ± 40	65 ± 7
SAU-FG-7	464 ± 56	48 ± 5
SAU-FG-8	928 ± 29	257 ± 28
SAU-FG-9	2633 ± 44	104 ± 12
SAU-FG-10	1520 ± 53	70 ± 8
SAU-FG-11	756 ± 61	47 ± 5
SAU-FG-12	1509 ± 53	52 ± 6
SAU-FG-13	91 ± 53	32 ± 4
SAU-FG-14	1758 ± 59	58 ± 6
SAU-FG-15	1615 ± 42	108 ± 12
SAU-FG-16	1679 ± 62	58 ± 7
SAU-FG-17	2391 ± 43	114 ± 13
DAG 476		
DAG-FG-1	352 ± 18	1110 ± 120
DAG-FG-2	750 ± 27	249 ± 28
DAG-FG-3	2347 ± 85	40 ± 5
DAG-FG-4	773 ± 21	492 ± 54

on Mg-rich and Fe-rich olivine. Vesiculation of feldspathic glass occurred, but is uncommon. The phase analyzed in SaU 005 is feldspathic glass (Table 7, Fig. 9).

3.8. Chassigny

Chassigny is the only known Martian dunite. It is composed of cumulate olivine (Fo_{66-69}), chromite, low-Ca pyroxene ($Mg_{69}Fe_{28}Ca_3$), and augite ($Mg_{46}Fe_{11}Ca_{43}$) with interstitial plagioclase. The plagioclase, unlike other Martian meteorites, did not undergo impact melting, but shows solid state shock metamorphic effects, such as fracturing, reduced birefringence, and planar deformation features. Fracturing and planar deformation features are also observed in olivine. Melt inclusions in olivine crystallized into augite, low-Ca pyroxene, a silica phase, and rarely apatite, chromite, and pyrrhotite. Most of these inclusions contain a residual magmatic glass (Fig. 1e). Small (2–10 μm) glass inclusions (Fig. 1f) are observed in some highly fractured olivine crystals. These inclusions may represent preexisting inclusions that were completely molten by impact. The phases analyzed in Chassigny are shocked plagioclase, apatite, magmatic glass in melt inclusions, and one glass inclusion in olivine (Table 8, Fig. 10).

4. RESULTS

4.1. ALH 84001

Four different water-bearing phases (whitlockite, chlorapatite, carbonate, and feldspathic glass) were found and analyzed by electron and ion microprobe (Table 2, Fig. 2). Of the minerals analyzed, the whitlockites have the lowest deuterium enrichments (91–441 ‰) and the most restricted range of isotopic compositions. The chlorapatite core in the zoned phosphate has a much higher δD (751±19 ‰) than the whitlockite

Table 8. The H isotopic compositions and water abundances of phases in Chassigny.

Sample	δD (‰)	H_2O (ppm)
Apatite		
CHAS-AP-1[a]	811 ± 23	2130 ± 90
Melt Inclusions		
CHAS-MI-1	185 ± 21	2740 ± 120
CHAS-MI-2	166 ± 23	1292 ± 82
CHAS-MI-3	95 ± 24	1940 ± 80
CHAS-MI-4	225 ± 20	3170 ± 170
Glassy Inclusions		
CHAS-GI-1	1754 ± 15	8550 ± 950
Shocked Plagioclase		
CHAS-SP-1	451 ± 50	53 ± 2
CHAS-SP-2	218 ± 22	923 ± 38
CHAS-SP-3	192 ± 22	711 ± 30
CHAS-SP-4	94 ± 22	2060 ± 190
CHAS-SP-5	684 ± 39	135 ± 5
CHAS-SP-6	598 ± 48	55 ± 2
Olivine		
CHAS-OL-1	−83 ± 77	88 ± 11

[a] This apatite was found in melt inclusion 1.

rimming it (135–297 ‰, Whitlockite 2 in Fig. 1). The $\delta^{18}O$ measurements are consistent with both the whitlockites (3.7–4.3 ‰) and apatite (5.1 ‰) being magmatic. The range of δD values in the carbonate grains appears to be related to their mode of occurrence. Small irregular carbonate grains disseminated in the cataclastic zones show lower δD values (147–290 ‰) relative to large irregular grains and zoned carbonate globules (331–1196 ‰). The δD values of the feldspathic glasses (1074–1738 ‰) are higher than those of the whitlockites and carbonates. The water contents of the glasses are generally low and exhibit at best a weak negative correlation with the δD values. Two analyses of one grain shows that the glasses can be quite heterogeneous (Fig. 2) and the variation between the two points parallels the general trend in the glass data. An unusually high water content in one area of glass (0.72 wt. %, δD=1074 ‰) may be due to the presence of layer lattice silicates (Brearley, 1998).

The distribution of REEs in whitlockite, the coexisting carbonate and clinopyroxene-rimmed orthopyroxene adjacent to them are shown in Figure 3. Whitlockite shows a LREE enrichment. A slight LREE enrichment is observed also for the clinopyroxene rims. Orthopyroxene is HREE-enriched and, given its abundance in the rock, it is the major HREE carrier in ALH 84001 (Wadhwa and Crozaz, 1998). The carbonate is also enriched in HREE. The feldspathic glass (Fig. 4) shows remarkable LREE enrichment and a positive Eu anomaly. The LREE enrichment found in the phosphate and feldspathic glass is in agreement with previous results (Wadhwa and Crozaz, 1998). The LREE enrichment of the clinopyroxene and whitlockite may be due to interaction with a LREE-enriched melt (Wadhwa and Crozaz, 1998) or late stage magmatic fluid.

4.2. EETA 79001 and ALHA 77005

The feldspathic glasses in EETA 79001 (Table 3 and Fig. 5) have δD values ranging between 1540 ‰ and 2753 ‰. The mafic glasses (δD=1697–2900 ‰) have, on average, higher D/H ratios than the feldspathic glass and also higher water contents.

The δD values of feldspathic glasses in ALHA 77005 (982–4214 ‰, see Table 4 and Fig. 6) overlap with those reported for feldspathic glasses in EETA 79001. We made only two measurements of mafic glasses in ALHA 77005: they gave δD values of 3030 ± 130‰ for the "pristine" mafic glass in one of

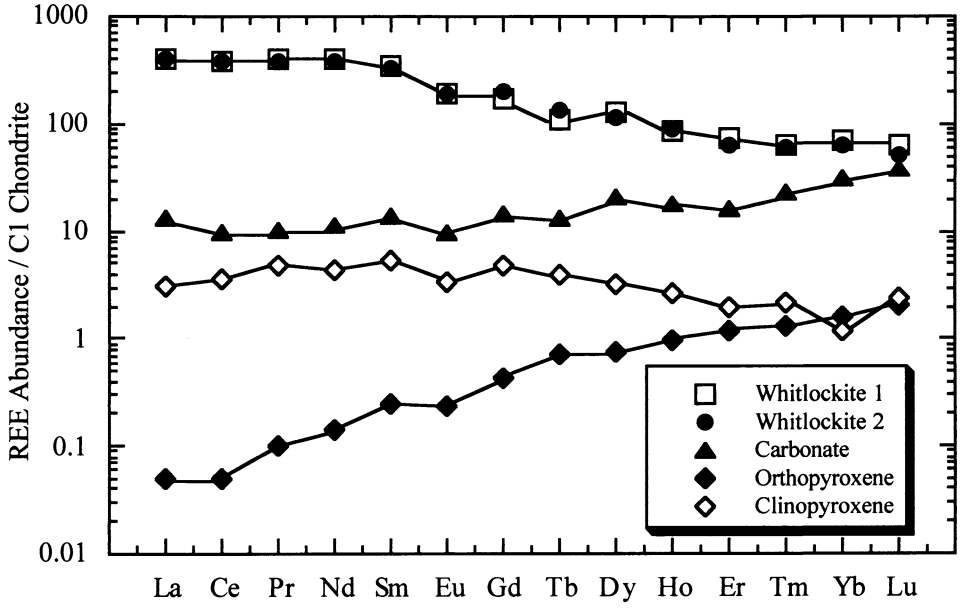

Fig. 3. The CI chondrite normalized rare earth element abundances in whitlockite and associated minerals in ALH 84001. The orthopyroxene, rimmed by clinopyroxene, is in contact with whitlockite 1. The carbonate is an inclusion in whitlockite 1. Abundances are normalized to the CI composition of Wasson and Kallemeyn (1988).

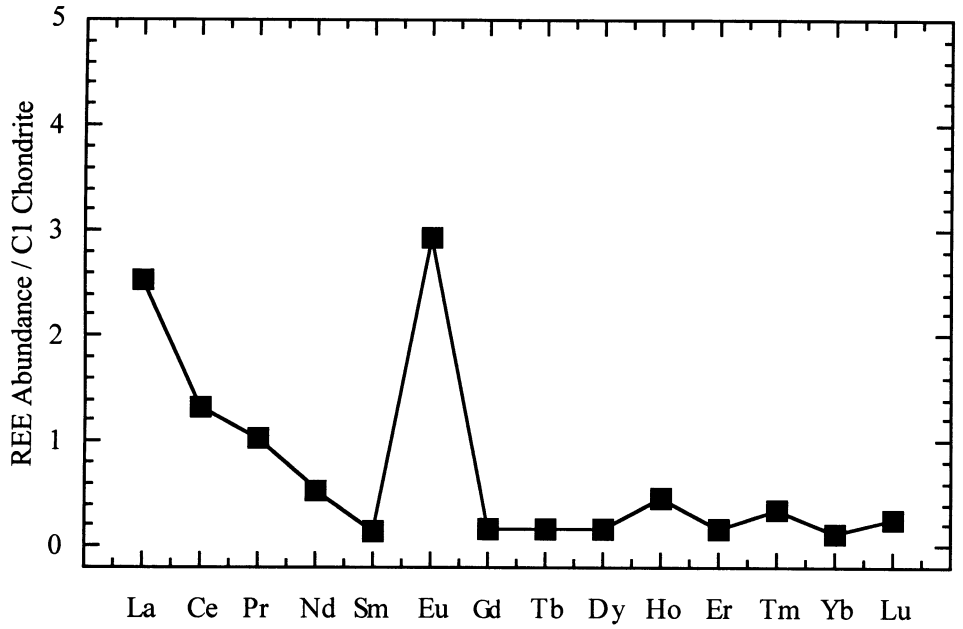

Fig. 4. The CI chondrite normalized rare earth element abundances in an area of feldspathic glass in ALH 84001. Abundances are normalized to the CI composition of Wasson and Kallemeyn (1988).

the melt pockets and 1301 ± 74‰ for devitrified glass in one of the melt veins. These results show that mafic impact melted glass, which forms at higher shock pressures than feldspathic glass, also has higher δD values. There is also a tendency for vesicular feldspathic glass to have somewhat higher δD relative to the nonvesicular glass.

The five ALHA 77005 melt inclusions analyzed fall into two groups. Three of the inclusions (77005-IN-1, -2, -3) have very low water contents (~1 ppm) that are similar to that of the one olivine analyzed. Water contents of <3 ppm in melt inclusions are almost certainly measurements of instrumental background. However, the slightly elevated δD values of 77005–1 and −2 (304 and 293‰, respectively) indicate that they do contain some indigenous water. The other group (77005-IN-4 and -5) have much higher water contents (357 and 1770 ppm, respectively) and low δD values.

4.3. Shergotty and Zagami

The δD values and water abundances of the water-bearing phases in these two meteorites are given in Tables 5 and 6, and Figures 7 and 8. The δD values of the feldspathic glasses in

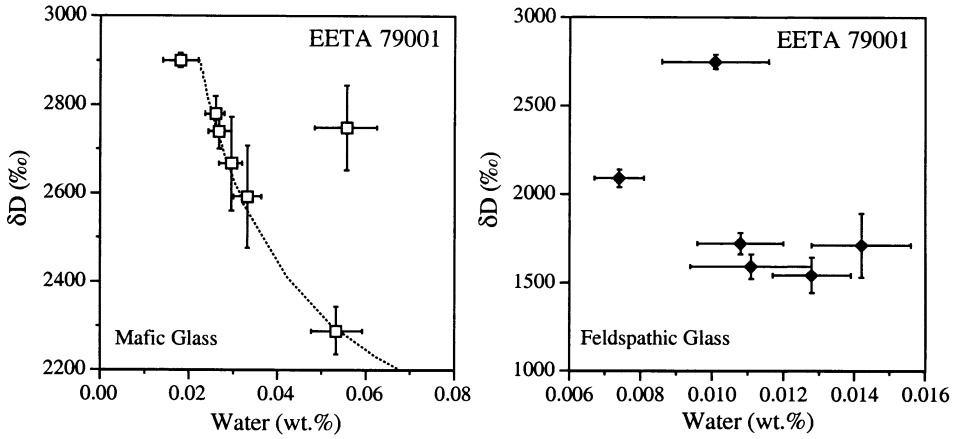

Fig. 5. The hydrogen isotopic compositions and inferred water contents of glasses in the meteorite EETA 79001. In the mafic glasses (Fig. 5a) there appears to be an approximate inverse correlation between δD values and water content, but there is no such relationship in the feldspathic glasses. Unlike in other meteorites, the range of glass compositions cannot be explained by mixing of a high δD component with a uniform water content, and an isotopically normal component. The mixing line in Figure 5a assumes that the high δD endmember (δD=2900 ‰, H_2O=164 ppm) mixes with a component that also has an elevated δD value (δD=1850 ‰).

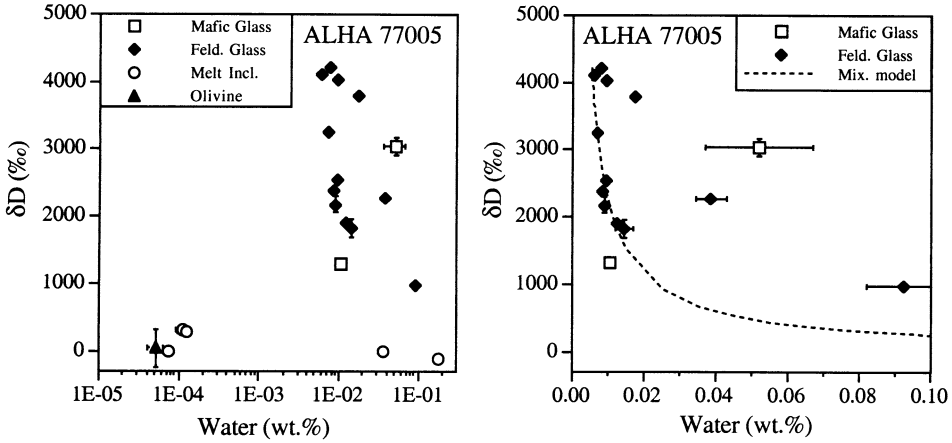

Fig. 6. The hydrogen isotopic compositions and inferred water contents of various components in the meteorite ALHA 77005. The mafic and the feldspathic glasses are very D-rich and exhibit considerable variation. The most D-rich areas have δD values like that of the present day Martian atmosphere. Most of the feldspathic glass compositions can be explained by mixing of a high δD component (δD≈4200‰, H_2O≈55 ppm) with a more abundant low δD component (δD≈0‰). Analysis of an olivine grain and three inclusions have very low water contents. These concentrations are close to the instrumental blank levels. Two other inclusions have relatively high water contents and low δD values.

Shergotty (−106 to 1577 ‰) overlap with those of Zagami (579–2282 ‰). The highest δD values (up to 2704 ‰) were found in the post-stishovite silica phase in Zagami. The post-stishovite silica phase in Shergotty has lower δD values (1246–1975‰) than in Zagami, but they are, on the average, higher than those of Shergotty's feldspathic glasses. In general, the silica-feldspathic glass intergrowths have lower δD values than the discrete post-stishovite silica or the feldspathic glasses.

In Zagami, there is a weak positive correlation between the δD values and water abundances in the feldspathic glasses, and all but one of the post-stishovite silica grains. The more water-rich silica-feldspathic glass intergrowths (4 grains) and one of the silica grains together suggest an inverse correlation between the δD value and water abundance.

4.4. Sayh al Uhaymir 005 and Dar al Gani 476

The δD values for feldspathic glasses in SaU 005 (Table 7, Fig. 9) range between –105 ± 17‰ and 3257 ± 41‰. There is also a positive correlation between the δD values and water abundances. In comparison, DaG 476 feldspathic glasses have lower δD values (352 ± 18 to 2347 ± 85‰). Although our data on DaG 476 are limited, there is an inverse correlation between the δD values and water abundances in the feldspathic glass.

4.5. Chassigny

The δD values and water abundances for shocked plagioclase, melt inclusion glasses, and a single apatite are given in

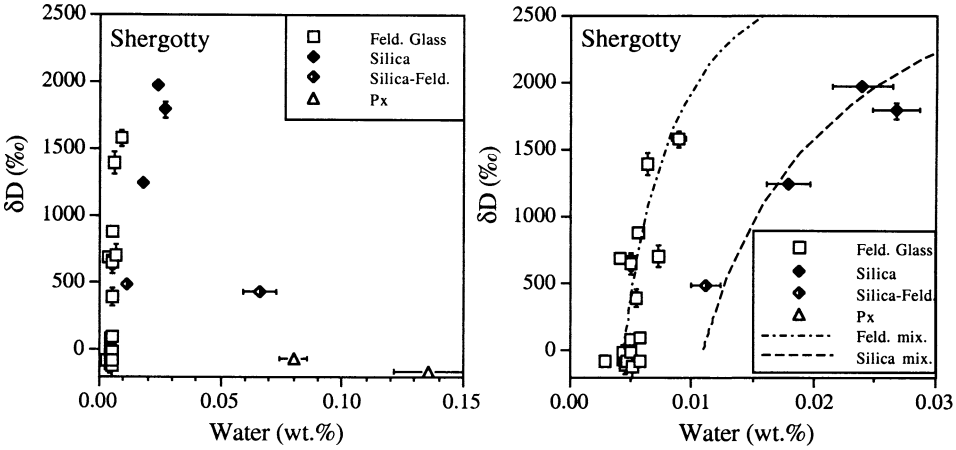

Fig. 7. The hydrogen isotopic compositions and inferred water contents of various phases in the Shergotty meteorite. Most of the feldspathic glass compositions are consistent with addition (Feld. Mix. line) of a high δD component (δD≈3500‰) to a low δD component with a fairly uniform abundance (δD≈0‰, H_2O≈50 ppm). The post-stishovite silica areas and one of the silica-feldspathic glass intergrowth regions require higher water contents for their low δD component (~180 ppm).

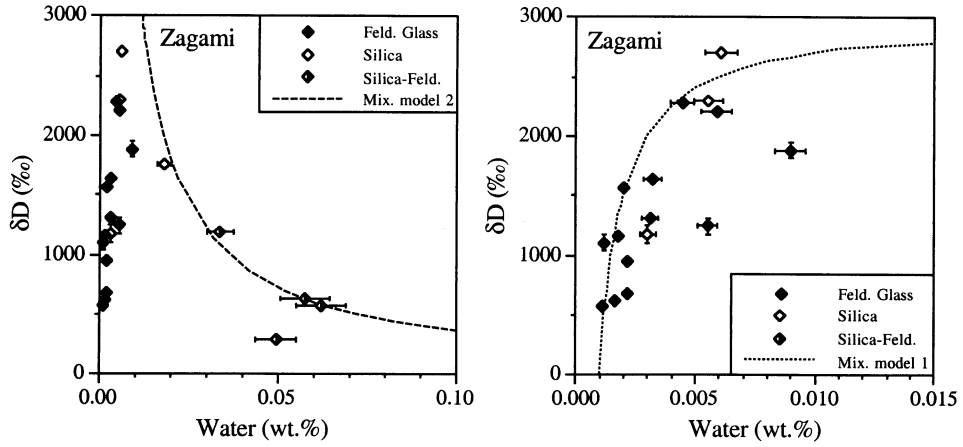

Fig. 8. The hydrogen isotopic compositions and inferred water contents of various phases in the Zagami meteorite. Most of the feldspathic glass compositions are consistent with addition (Mix model 1) of a high δD component (δD≈3000‰) to a low δD component with a uniformly low abundance (δD≈0‰, H_2O≈12 ppm). Three of the pure post-stishovite silica polymorph areas may require somewhat higher water contents to explain their low δD component. The three silica-feldspathic glass intergrowth regions, as well as one of the pure post-stishovite silica areas show an inverse correlation between their δD values and water contents, consistent with the addition of isotopically normal water to a high δD component with a fairly uniform concentration (δD≈3000‰, H_2O≈175 ppm).

Table 8 and plotted in Figure 10. The δD values for shocked plagioclase range between 94 ‰ and 684 ‰. There is an inverse correlation between the δD values and water abundances. The magmatic melt inclusion glasses have δD values between 90 ‰ and 184 ‰. In contrast, the one small glassy inclusion that has been measured is more enriched in D (δD=1754 ± 15‰). An apatite crystal found in one of the melt inclusions has a δD value of 834 ‰, compared to 185 ‰ for the inclusion's glass.

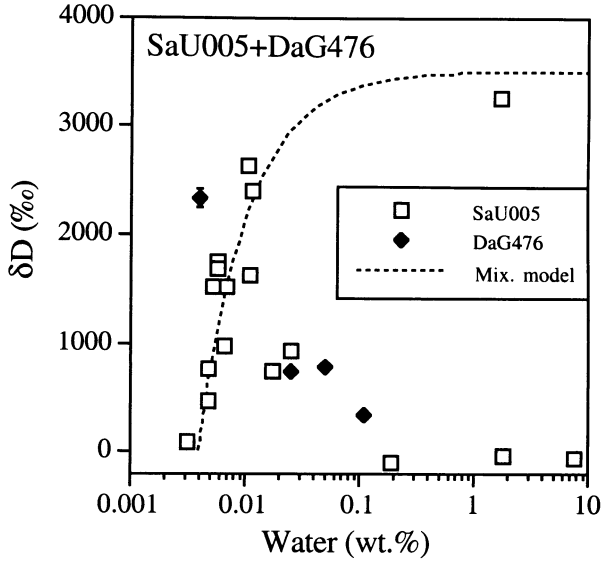

Fig. 9. The hydrogen isotopic compositions and inferred water contents of feldspathic glasses in the meteorites SAU 005 and DaG 476. Most of the feldspathic glass compositions in SAU 005 are consistent with addition (Mix. model) of a high δD component (δD≈3500‰) to a low δD component with a fairly uniform abundance (δD≈0‰, H_2O≈40 ppm). The remaining SAU 005 glasses and the glasses from DaG 476 seem to fall on a trend with δD inversely correlating with water content, i.e., mixing of a high δD component (δD≥2350‰, H_2O≤50 ppm) with a more abundant low δD component (δD≈0‰).

5. DISCUSSION

The hydrogen isotopic compositions of the water-bearing phases in the meteorites we studied, though variable, differ significantly from the hydrogen isotopic signature of terrestrial materials (δD –300‰ to 100 ‰), confirming that they all contain at least some water of extraterrestrial origin. Similar observations were made by Leshin et al. (1996) for the whole rock SNC meteorites, and for kaersutite and apatite in Chassigny and Shergotty (Watson et al., 1994). The more striking results of this study are: (1) the very high δD values found in some phases, and (2) the range of compositions we observe, even within a single meteorite. Such large ranges in H isotopic compositions are not unique to our study. In ALH 84001, Sugiura and Hoshino (2000) found similar ranges for the same phases analyzed here, although they report somewhat higher maximum values. Watson et al. (1994) found a 1000 ‰ variation in a single apatite from Zagami, and a similar range in kaersutites from Chassigny. Finally, Leshin (2000) reports an almost 2000 ‰ variation in apatite grains from QUE 94201. Below, we examine what could have produced the high δD values, as well as the ranges reported here and in these previous studies. In particular, we examine the possible roles of terrestrial contamination, of interaction with the Martian exchangeable reservoir, and of shock devolatilization during impact.

5.1. Terrestrial Contamination

We are unable to distinguish between low δD Martian and terrestrial waters. However, several lines of evidence point to variable terrestrial contamination as an explanation for much of the range of isotopic compositions observed within and between meteorites. Many of these can be illustrated with the

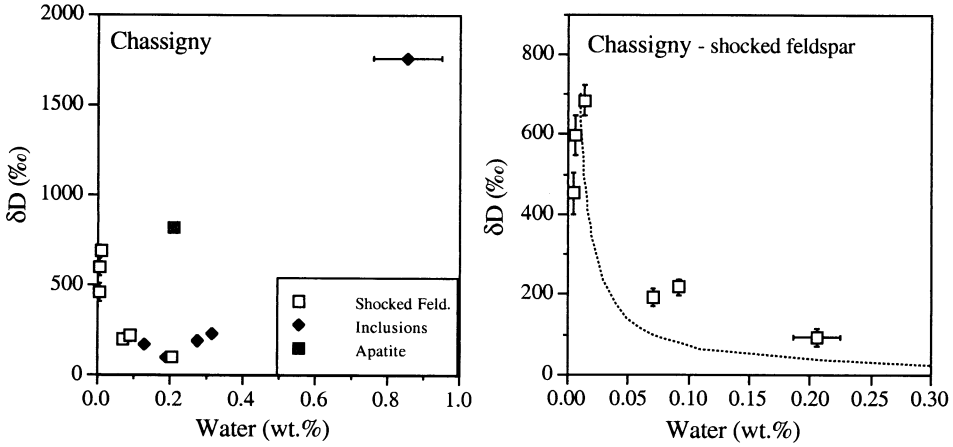

Fig. 10. The hydrogen isotopic compositions and inferred water contents of various components in the Chassigny meteorite. The range of feldspathic glass compositions can be explained by mixing of a high δD component with a more abundant low δD component. The compositions for the mixing line in Figure 10b are δD≈700‰, and H_2O≈100 ppm, and δD=0‰. The fact that the more water-rich points fall above the mixing line suggests that either the high δD endmember has a variable water concentration and/or it has mixed with a component that also has a slightly elevated δD value. All but one of the melt inclusions have relatively low δD values and modest water contents that are similar to the most water-rich feldspathic glasses. One melt inclusion has a very high water content and δD value. Its isotopic composition is close to the highest value reported for kaersutite in Chassigny inclusions (Watson et al., 1994), but kaersutite was not observed in this inclusion.

results of this and other studies of ALH 84001. All of the Martian meteorites examined by Leshin et al. (1996) using step-wise heating released significant amounts of terrestrial water below 350 °C. In the case of ALH 84001, ~70% of the water is released below 350°C. Also, Jull et al. (1995, 1998) report evidence for terrestrial carbonate and organic matter contamination in ALH 84001. We also observed a correlation between δD and grain size in our ALH 84001 carbonate analyses. The lowest δD values are found in fine-grained, irregular carbonate in the cataclastic zones, whereas the highest values are for the zoned carbonate globules. In the sections of ALH 84001 made available to us, the carbonate globules were not as large or as well developed as have been reported elsewhere. This may explain the higher δD values in ALH 84001 carbonates reported by Sugiura and Hoshino (2000). In addition, the fact that the δD values rose significantly during the course of many analyses demonstrates that there has been surface contamination of the sections. Although we are unable to distinguish between low D Martian and terrestrial water, we are more inclined to attribute the large range in δD in ALH 84001 carbonates to mixing of extraterrestrial and terrestrial components.

As some or all of the carbonates in ALH 84001 probably have been terrestrially contaminated and the phosphates are generally heavily fractured, variable terrestrial contamination again seems the likely explanation for the range of D/H ratios we observe in the phosphates of ALH 84001. The fact that the one apatite grain we analyzed has a higher δD (751 ‰) than the surrounding rim of whitlockite (135–297 ‰) supports this conclusion.

Two patterns have emerged from our data for the feldspathic glasses and silica phases. These two patterns probably reflect two distinct processes. Both processes seem to have effected all the samples to varying degrees, complicating interpretation of the data. The first of these patterns is best seen in Zagami, Shergotty and SaU 005 (Figs. 7–9). In these meteorites, feldspathic glasses and post-stishovite silica with low water contents exhibit a positive correlation between δD value and inferred water content. This positive correlation seems to result from a mixing between two components: a nearly constant abundance of a component with low water content and low δD (~0‰) to which a high δD (~3000–4000‰) component is being added. The high δD is almost certainly fractionated Martian water. The origin of the low δD material is more problematic. Its low water concentration (12–150 ppm), variations between meteorites, and nearly constant abundance in a given phase in a meteorite suggests that it is not our instrumental blank. It is either contamination of the meteorites/sections, or it could be Martian magmatic water inherited from the preshocked minerals.

The second pattern, almost the reverse of the first, is best seen in the feldspathic and mafic glasses of ALH 84001, ALHA 77005, and EETA 79001 (Figs. 2, 5 and 6), as well as in the silica-feldspathic glass intergrowths of Zagami. In these samples, there is an inverse correlation between δD and water content. This seems to be due to addition of a low δD component to a high δD (3000–4000‰) component of fairly constant concentration. This is very similar to the pattern observed in QUE 94201 phosphates by Leshin (2000). However, we find in the meteorites we have studied that, except for EETA 79001, the low δD component is probably closer to 0 ‰ rather than 900 ‰ as Leshin (2000) found in QUE 94201. At present, our preferred explanation for both these low δD components is that they are terrestrial contaminants, but we cannot rule out the presence of a low D Martian magmatic component.

Recently, Gillet et al. (2002) reported negative δD values ranging from –60 to –280 ‰ in olivine and pyroxene and from –140 to –181 ‰ for an alteration phase in the nakhlite NWA 817. They suggested that the alteration in NWA 817 was likely produced on Mars by the circulation of an aqueous fluid orig-

inating from a chemical reservoir, such as the upper mantle, which has not equilibrated with a fractionated Martian atmosphere. Our investigation of H isotope signatures of the nominally anhydrous minerals in the nakhlites Nakhla and Governador Valaderes (Boctor et al., 2002) show that clinopyroxene has a fractionated H isotope signature ($\delta D = 572-830$ ‰ and 103–1243 ‰ for Nakhla and Governador Valaderes, respectively.) The range of D/H ratios in the clinopyroxenes suggests that they are mixtures of a low D component and a highly fractionated H component. The highly fractionated H component was derived from the Martian exchangeable reservoir. The low D component may be a Martian magmatic component or a terrestrial contaminant. We cannot conclusively distinguish between these two low D end members in our nakhlite sample, nor do we believe that terrestrial contamination of NWA 817 can be ruled out.

5.2. Interaction with the Exchangeable Reservoir

Given the ambiguity in the interpretation of the low δD values, for the remainder of this paper we concentrate on the origin of the highest δD values, particularly those in the feldspathic and mafic glasses, and the post-stishovite silica in the shergottites. The conventional interpretation of the high δD values in Martian meteorites is that they reflect interaction with water from the exchangeable reservoir. In EETA 79001, Shergotty and Zagami, modern Martian atmospheric gases were implanted into the shock melts (e.g., Bogard and Johnson, 1983; Marti et al., 1995; Bogard and Garrison, 1998; Garrison and Bogard, 1998). Modern Martian atmospheric gases were also found, although at lower concentrations, in olivine and pyroxene separates from ALHA 77005 (Garrison and Bogard, 1998). Presumably, shock melting promotes trapping of these gases. The glasses and mineral separates also contain trapped noble gases from the Martian interior and the terrestrial atmosphere. The presence of three noble gas components is intriguing because they may well have been accompanied by water and three components may be needed to explain all our H isotope data.

Un-like the above meteorites, Chassigny contains little or no Martian atmospheric noble gases and a mantle N isotope signature (Mathew and Marti, 2001). Indeed, its noble gases appear to be dominated by the Martian interior component (Ott, 1988; Swindle, 1995). Chassigny experienced the lowest shock pressures of the meteorites we have studied. It did not experience shock melting, except for the tiny, glassy melt inclusions in heavily fractured olivines that probably formed by impact melting. If, as seems likely, shock melting played an important role in introducing the noble gases and, possibly, high δD water into the meteorites, one would expect that less shocked meteorites would have lower Martian atmospheric signatures, both in the noble gases and the δD values of their water. The low δD values in the Chassigny shocked plagioclase we have measured (94–684 ‰) are consistent with this suggestion (Table 8, Fig. 10). The one Chassigny apatite grain we have measured also has a fairly low δD value (811 ‰) compared to apatites from shergottites (Watson et al., 1994; Leshin, 2000).

The four Chassigny melt inclusions measured have low δD values (95–225 ‰) and modest water contents (0.1–0.3 wt.%). This contrasts with the high δD value (1754 ‰) and higher water content (0.85 wt.%) of the small glassy inclusion. The low δD values of the melt inclusions and the noble gas data for bulk Chassigny suggests the intriguing possibility that these inclusions have retained a primary magmatic signature. The low δD values are also consistent with the low δD value for the bulk meteorite reported by Leshin et al. (1996). However, our observation of the one glassy inclusion with both a high δD and high water content, and the high δD for kaersutite in Chassigny inclusions (Watson et al., 1994), requires explanation and will be discussed further in the section on melt inclusions.

ALH 84001 did experience shock melting of its feldspar. However, the glasses in ALH 84001 are not rich in noble gases or nitrogen (Grady et al., 1998), suggesting that the water in the glasses was not atmospheric. More likely it was subsurface water from exchangeable reservoir. If the highest δD water in the glasses reflects that of the exchangeable reservoir when they formed 3.9 Gyr ago (Ash et al., 1996), the most deuterium-rich compositions provide lower limits (~1750 ‰) for the composition of the Martian atmosphere at that time. This would imply either an initially high δD value for Mars (e.g., Leshin, 2000), and/or a rapid loss of water and associated H isotopic fractionation early in Mars's history. Assuming that the maximum δD value of the glass in ALH 84001 was the composition of the atmosphere at 3.9 Gyr, estimates of the volume of the exchangable reservoir at that time, based on (1) hydrogen loss rates since 3.9 Gyr and (2) the amount of water that must have been lost before 3.9 Gyr, are broadly consistent with the volumes estimated from post-Noachian outflow channels and ocean (see appendix for details).

However, there is little evidence of a systematic variation with time of the atmospheric/exchangable reservoir H isotopic composition, as estimated from the maximum δD values measured in or inferred from the meteorites (see Table 9). An early Martian atmospheric signature is indistinguishable from that produced by mixing of a terrestrial water reservoir and the present-day Martian atmosphere, or the current Martian atmosphere with magmatic water on Mars. We cannot rule out that ALH 84001 interacted with a Martian water reservoir with a present-day D/H ratio and the measured δD values of the glasses reflect mixing of water with fractionated Martian composition and terrestrial contamination. This would have to be achieved without resetting the Pb-Pb and Ar-Ar ages of the carbonates and glasses, respectively, but this may be possible given that H is significantly more mobile than Ar or Pb.

5.3. Isotopic Fractionation during Shock Metamorphism?

The fact that the highest δD values were measured in the impact melted glasses and the high pressure post-stishovite silica suggests an additional potential complication in the interpretation of the H isotopes: i.e., that shock metamorphism may have played a role in producing the H isotope fractionation observed in these phases. Most of the feldspathic glasses in the studied meteorites formed by shock melting at pressures of ~ 35–40 GPa. Vesiculation in the feldspathic glass (ALHA 77005 and EETA 79001) would require a minimum peak pressure of ~45 GPa. Formation of mafic glass by impact melting requires a minimum shock pressure of ≥60 GPa. Extensive whole rock shock melting (EETA 79001, lithology A) would require shock pressures in excess of 60 GPa. There is

Table 9. Summary of some of the features of the meteorites and measurements. These include ages of the meteorites, estimates of the maximum localized peak shock pressures they experienced, their bulk δD values measured by stepped heating, maximum δD values measured here, and maximum δD values inferred from data presented here or from other sources.

	Age[a] (m.y.)	Shock P. (GPa)	Bulk δD[b] (‰)	Max δD (‰)	Infer. δD (‰)
Zagami	185 ± 25	≥40	1102	2704	≥4000[c]
Shergotty	185 ± 25	≥40	1174	1975	~3500
EETA 79001	174 ± 3	~60–80[d]	1472	2900	≥2900
ALHA 77005	187–154	~60–80[e]		4214	≥4200
SaU 005	700	>60		3257	~3500
DaG 476	700	~40		2347	≥2350
Chassigny	1300	~25	−48 to 26	1754	≥1880[c]
ALH 84001	3900[f]	~40	573	1738	≥2100[g]

[a] From the compilation of McSween and Treiman (1998) and references therein.
[b] >350°C steps from Leshin et al. (1996).
[c] From Watson et al. (1994).
[d] Localized shock melting that produced lithology C. The plagioclase glasses in lithology B would have formed at 35–40 GPa.
[e] Localized conditions that produced textured regions. The plagioclase glasses would have formed at 35–40 GPa.
[f] Age of the feldspathic glass and carbonates where the highest δD values have been found.
[g] From Sugiura and Hoshino (2000).

some uncertainty about the conditions needed to form the post-stishovite silica. The αPbO_2 silica phase is stable at 82 GPa and 970 K (Dubrovinsky et al., 2001). When heated at 960 K at a pressure of 58 GPa, it inverts to stishovite. When tridymite was used as starting material, transformation to the post-stishovite silica occurred at 45 GPa at ambient temperature (Dubrovinsky et al., 2001).

To summarize, the meteorites studied were shocked at pressures of ~40 GPa to ≥60 GPa (Table 9). It seems unlikely that the H isotopes would remain completely unaffected when the host meteorites were subjected to such extreme pressures and the accompanying high temperatures. The question is, how large an influence could shock-induced isotopic fractionation have been?

In a series of experiments, Tyburczy et al. (1990) found that the water remaining in shocked samples was isotopically heavy, and they inferred that water was lost primarily from shock-melted regions. They also found that the isotopic fractionation factor changed with increasing shock pressure, suggesting that at low shock pressures (<10 GPa, T=1500 K) water is the dominant species to be lost whereas at higher shock pressures and temperatures (20–30 GPa, T~1500–2000 K) H_2 dominates. Extrapolation of their results to conditions that are more appropriate to Martian meteorites suggests that atomic hydrogen will become dominant. The isotopic fractionation as a function of degree of hydrogen loss is greatest when atomic hydrogen dominates.

These experiments suggest that impact melting induces devolatilization of H and an associated D enrichment of the melt. The solubility of water in feldspathic melts rises dramatically with pressure, reaching 10–15 wt.% water at 1 GPa (Silver and Stolper, 1989). The water contents of the impact glasses in the meteorites are now low, but if they approached 10–15 wt.% at the peak of the shock, this would imply considerable water loss and associated D enrichment. Variable hydrogen loss via a Rayleigh-type process from individual melt pockets (i.e., little exchange between them) would produce a clear inverse relationship between water abundance and δD. The evidence for such a relationship in our data is weak, although there are hints of one in the feldspathic glasses in ALH 84001, the silica-feldspar glasses of Zagami and the mafic glasses of EETA 79001. There is little physical evidence (e.g., widespread vesiculation) for the loss of large amounts of water from these glasses. However, preservation of vesicles will depend on the super-solidus cooling history of the glasses.

Recently, Tyburczy et al. (2001) reported shock-related isotopic fractionation in experiments with the Murchison meteorite, but concluded that shock cannot produce very large positive δD values, such as that of the present day Martian atmosphere. It is likely, therefore, that the water incorporated in the glass was primarily fractionated surface or underground water, although some additional D enrichment may have occurred by devolatilization of H from the impact melt.

A third possible mechanism by which fractionated H may be incorporated in the glasses is shock implantation of H from the Martian atmosphere. This process could be particularly important in meteorites where the impact glasses show evidence of trapped Martian atmosphere noble gases, e.g., Shergotty and Zagami.

The carbonates in ALH 84001 may provide clues that help to determine if shock has played a role in fractionating the hydrogen isotopes. If the carbonates were melted by shock or were even partially vaporized (Scott, 1999), shock-induced fractionation could have produced or enhanced their observed deuterium enrichment.

Shock experiments (Lange et al., 1985; Tyburczy et al., 1986) show that carbonates undergo decomposition and volatile loss during dynamic compression. Osinski and Spray (2001) also described calcite globules in the Haughton impact structure which they interpreted as impact melts. Recent investigation of the carbonates in ALH 84001 by transmission electron microscopy (Barber and Scott, 2002) show that magnesite partially decomposed to periclase (MgO), and that the sideritic and ankeritic carbonates have also undergone impact induced decomposition to form the magnetite-rich rims. These observations by Barber and Scott are consistent with shock-induced D enrichment by H loss during impact. Decomposition and loss

of CO_2 could also have affected the C and O isotopic compositions of the carbonates.

However, at present the most widely accepted view is that the carbonates post date the shock event which produced the feldspathic glasses (Treiman, 1998) and that they precipitated from a fluid at relatively low temperatures or from brines (Valley et al., 1997; Treiman and Romanek, 1998; Warren, 1998). Eiler et al. (2002) suggest that the H carrier phase(s) is a refractory hydrous salt, such as hydromagnesite. In this case, shock cannot have played a role in producing the high δD values of the carbonates. Rather, their high δD values require that the fluid they formed from came from the exchangeable reservoir, unless multiple shock events affected ALH 84001 and the latest event postdated the carbonate precipitation. Treiman (1995) has suggested that two shock events effected ALH 84001, and the second postdates the precipitation of carbonates from fluids.

5.4. Melt Inclusion Glasses

In both Chassigny and ALHA 77005, the residual magmatic glasses in melt inclusions have relatively low δD values (≤300 ‰), but a wide range of water contents (1–3200 ppm). In Chassigny, however, the one small (≤10 μm) silica-rich, glassy inclusion in an intensely fractured olivine is significantly enriched in D (δD=1754 ‰). If one assumes that the glasses from both types of inclusion interacted with a fractionated Martian water reservoir, much more extensive terrestrial contamination must be invoked to explain the low δD values of the residual magmatic glasses. It is difficult to explain why the glasses in these large inclusions are affected by terrestrial contamination, whereas the smaller glassy inclusion preserved a highly fractionated isotopic signature. In fact, the reverse might be expected, because the extensive fracturing of the host olivine makes the glassy inclusion more accessible to terrestrial water.

A more likely explanation for the fractionated H isotope signature of the glassy inclusions is that when they were impact melted they incorporated fractionated Martian water and/or H was fractionated during shock induced devolatilization. If that is the case, then the low δD values of the glass in the magmatic melt inclusions may represent a close approximation of the primary magmatic signature on Mars. However, the high δD values of apatite and kaersutite in the magmatic melt inclusions of Chassigny (Watson et al., 1994) are problematic for this explanation. These phases almost certainly have partially equilibrated with a D-rich water reservoir on Mars. If the inclusion glasses retain a primary magmatic signature, we are forced to conclude that exchange with apatite and kaersutite, which already have OH sites in their structure, was kinetically favored relative to the glasses. If primary, the relatively modest water content of the magmatic melt inclusion glasses suggests that either the water content of the parent magma was low or the magma was degassed before the entrapment of the inclusions.

5.5. Preservation of Primary H Isotope Signature in Apatite?

If the low δD signatures of the glasses in the melt inclusions are magmatic signatures, the primary H isotope signature of Mars is not very different from that of Earth. However, Leshin (2000) argued on the basis of measurement of hydrogen isotopes in apatite from Martian meteorite QUE 94201 that the pre-Jeans escape Martian water reservoir had a D/H value twice that of terrestrial water, concluding that the current remaining amount of water in the Martian reservoir is two to three times higher than previously thought in models that assumed an initial Martian D/H signature similar to that of Earth.

The δD values reported here for whitlockite and apatite in various meteorites are typically much lower than for the respective feldspathic glasses in the same meteorite, which we suggest probably results from greater terrestrial contamination of the phosphates. We do find δD values of 751‰ and 811‰ for chlorapatite grains in ALH 84001 and a Chassigny melt inclusion, respectively. However, it is not clear whether these compositions represent the magmatic component or an atmospheric hydrogen component mixed with considerable terrestrial contamination. The one apatite grain measured in EETA 79001 has a δD value of only 146‰.

QUE 94201 is an Antarctic find. Therefore, the possibility that the anticorrelation between the δD values and the water abundances in QUE 94201 apatites reported by Leshin (2000) is influenced by terrestrial contamination cannot be excluded. The apparent relationship the δD values and the water abundance does not allow for a simple addition of terrestrial contamination to apatite with a uniform initial water content. However, we note that the range of compositions could be explained by adding water with δD=0 ‰ to apatites with an initial range of water contents of 0.18−0.27 wt. % and a δD=4200 ‰. The addition of water could be achieved by halogen-OH exchange, for instance.

We have measured feldspathic glasses and apatite grains in one section of QUE 94201, but do not report them in full here because the section was cut very close to the fusion crust. Nevertheless, Figure 11 illustrates some of the problems we encountered in measuring apatites in this meteorite. During the course of their analyses, two of the apatites show a very clear inverse correlation between δD values and water contents. This behavior can be closely modeled in terms of mixing between a high δD component (~2500‰ and 75 ppm) to which water with a composition of 0 ‰ is being added. The largest change in δD value (~2000 ‰) is accompanied by a modest rise in the Si^-/O^- ion ratio, suggesting that the ion beam is sputtering into increasing amounts of water-rich silicate material. The third apatite grain exhibits a similar range of Si^-/O^- ion ratios, but its δD values remain constant, presumably because the H isotopic composition of the apatite is similar to that of the silicates. The similarity of the H isotopic composition of this apatite to the silicates probably indicates almost complete exchange with terrestrial water.

The δD value measured can, therefore, be very sensitive to the amount of silicate material (or other contaminants) inadvertently included in an analysis. In the analyses in Figure 11, the beam is increasingly sputtering into silicate material. If the silicates were inclusions or embayments in an apatite, one might see a similar effect. Apatites analyzed with slightly different amounts of silicate material will produce an inverse correlation between δD and water content. With the exception of one area (δD≈3000 ‰), the feldspathic glasses had δD values of −250 ‰ to 580 ‰. If the δD values of the silicates

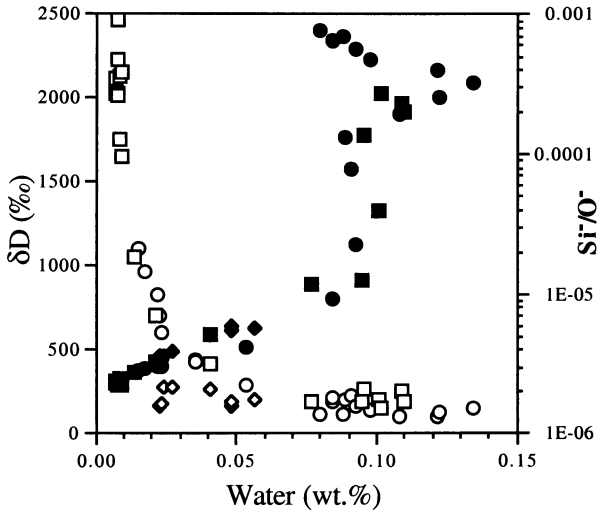

Fig. 11. The variation in δD values (open symbols) and Si^-/O^- ion ratios (filled symbols) with water contents during the analyses of three apatites in QUE 94201. Two of the apatites exhibit a strong inverse correlation between δD values and water content, which can be modeled assuming water with an isotopic composition of about δD≈0 ‰ is being added to a high δD component (~2500 ‰, ~75 ppm). Based on the correlated variations of the Si^-/O^- ion ratios, this mixing appears to be due to the ion beam sputtering into water-bearing silicate material underlying the apatites. The third apatite has a uniformly low δD value during the analysis, presumably because this apatite has a similar isotopic composition to the silicates.

in more interior parts of QUE 94201 are more D-rich (less contaminated), the low δD component in the mixing curve would not be at 0 ‰, but at some higher value. However, the apatite grains measured by Leshin (2000) are more water-rich than the apatites we measured. To produce the inverse correlation between δD and water content reported by Leshin (2000) by contamination with silicates, the surrounding silicates would have to be more water-rich than any we have found in our section of QUE 94201.

Because of the implications of using the H isotope signature of apatites to estimate the D/H of the Martian reservoir on the water budget of Mars, we must also evaluate whether apatite is likely to preserve a primary magmatic hydrogen isotopic signature.

Apatite in Martian meteorites is a chlorapatite. Diffusional exchange of Cl and OH is rapid, particularly along the C-axis, to the extent that it would begin to affect the core of a 50 μm apatite crystal in 6 days in the presence of an aqueous fluid at 800 °C (Brenan, 1993, 1994). At temperatures as low as 400°C, the core of the same size crystal will begin to exchange its halogens for OH in <25000 yr, a geologically reasonable time scale at this temperature. Brenan (1994) noted that some of the apatites in the exchange experiments showed heterogeneity in OH distribution. He attributed this heterogeneity to rapid migration of H through the apatite lattice accompanied by formation of an equivalent amount of an oxyapatite component (O^{2-}) in hydroxyl sites, a mechanism first proposed by Skinner et al. (1975). Hydroxyapatite starts to dehydrate at about 705°C (Skinner et al., 1975). On the other hand, Nadeau et al. (1999) found that to fully extract the water from fluorine-bearing apatites required heating times on the order of one day at temperatures of 1500°C. Perhaps, the presence of fluorine extends the thermal stability of apatite to higher temperatures. Also, Nadeau et al. (1999) did not determine the water loss as a function of time at 1500°C or at lower temperatures. Consequently, partial water loss probably happens on faster time scales even at lower temperatures than 1500°C. Nevertheless, temperatures higher than 1500°C can be reached locally during impact heating.

The geologically rapid rates of Cl-OH exchange demonstrated in these experiments suggest that the exchange may even occur during interaction of apatite with surface water on Mars and during Antarctic weathering (which is supported by the QUE apatite with the very modest D enrichment) over geologically reasonable time scales. This is particularly true if shock heating has dehydrated the apatite to some extent. Therefore, apatite may not be the "inert" mineral that preserves the initial isotopic signature of its parent magma and, like other phases, it should be used with caution.

6. CONCLUSIONS

The H isotope signatures of the carbonate, phosphate, shocked plagioclase, post-stishovite silica, impact melted feldspathic and mafic glass in six shergottites, Chassigny, and ALH 84001 show that all these meteorites contain an extraterrestrial hydrogen component. All the Martian meteorites studied contain phases with much higher δD values compared to their whole rock δD values. Chassigny is an extreme case; it has a terrestrial whole rock H isotope signature, but contains D-enriched apatite, kaersutite, and glassy melt inclusions.

No single mechanism can explain the range of D/H ratios observed in the different phases in these meteorites. The initial magmatic D/H ratios and water abundances have been modified by three mechanisms: terrestrial contamination, exchange with a fractionated Martian reservoir, and devolatilization of hydrogen by impact melting.

The positive correlation observed between δD and water abundance in feldspathic glass and post-stishovite silica in Zagami, Shergotty, and SaU 005 suggest mixing of a high δD component (3000–4000‰) with a low δD (~0‰) component that is either a terrestrial contaminant or a magmatic Martian component. The negative correlation between δD and water abundance in feldspathic and mafic glass, in ALH 84001, ALHA 77005, and EETA 79001 is consistent with addition of a low δD terrestrial contaminant to a high δD component. In both cases, the high δD component is fractionated Martian water.

Determination of the H isotope compositions of magmatic glass from melt inclusions in Martian meteorites may help constrain the initial H isotope signature of Mars. The low δD values reported here for magmatic glass in most melt inclusions that have not been shock melted may approximate the magmatic H isotope signature of Martian parent magma. If this is the case, the signature is not unlike that of bulk Earth.

Acknowledgments—Partial support for this research was provided by the NASA Astrobiology Institute and the Center for High Pressure Research (CHIPR). We would like to thank M. Lindstrom, T. McCoy, G. MacPherson, G. Kurat, and J. Zipfel for providing the samples. Reviews by M. Wadhwa, E. Deloule, and C. Koeberl helped to greatly improve the manuscript.

Associate editor: C. Koeberl

REFERENCES

Alexander C. M. O'D. (1994) Trace element distributions within ordinary chondrite chondrules: Implications for chondrule formation conditions and precursors. *Geochim. Cosmochim. Acta* **58**, 3451–3467.

Ash R. D., Knott S. F., and Turner G. (1996) A 4-Gyr shock age for a martian meteorite and implications for the cratering history of Mars. *Nature* **380**, 57–59.

Barber D. J. and Scott E. R. D. (2002) Origin of supposedly biogenic magnetite in the Martian meteorite Allan Hills 84001. *Proc. Nat. Acad. Sci.* **99**, 6556–6561.

Bischoff A. and Stöffler D. (1992) Shock metamorphism as a fundamental process in the evolution of planetary bodies: Information from meteorites. *Eur. J. Mineral.* **4**, 707–755.

Bjoraker G. L., Mumma M. J., and Larson H. P. (1989) Isotopic abundance ratios for hydrogen and oxygen in the Martian atmosphere. *Bull. Am. Astron. Soc.* **21**, 991 (abstr.).

Boctor N. Z., Fei Y., Bertka C. M., Alexander C. M. O'D. and Hauri E. (1998a) Vitrification and high pressure phase transition in olivine megacrysts from lithology A in Martian meteorite EETA 79001. *Lunar Planet. Sci. XXIX*. Lunar Planet. Inst., Houston. #1492 (abstr.).

Boctor N. Z., Fei Y., Bertka C. M., Alexander C. M. O'D., and Hauri E. (1998b) Shock metamorphic features in lithologies A, B and C of Martian meteorite Elephant Moraine 79001. *Meteoritics Planet. Sci.* **33**, A18 (abstr.).

Boctor N. Z., Fei Y., Bertka C. M., Alexander C. M. O'D. and Hauri E. (1999) Shock metamorphic effects in Martian meteorite ALHA 77005. *Lunar Planet. Sci. XXX*. Lunar Planet. Inst., Houston. #1628 (abstr.).

Boctor N. Z., Alexander C. M. O'D., Wang J. and Hauri E. H. (2001) Hydrogen isotope studies of water-bearing post-stishovite silica phase and feldspathic glass in the Martian meteorites Shergotty and Zagami. *Lunar Planet. Sci. XXXII*. Lunar Planet. Inst., Houston. #1309 (abstr.).

Boctor N. Z., Wang J., Alexander C. M. O'D., and Hauri E. (2002) D/H of minerals and melt inclusions in the SNCs Nakhla and Governador Valadares meteorites.. *Meteoritics Planet. Sci.* **37,** *Suppl,* A19 (abstr.).

Bogard D. D. and Garrison D. H. (1998) Relative abundances of argon, krypton, and xenon in the Martian atmosphere as measured in Martian meteorites. *Geochim. Cosmochim. Acta* **62**, 1829–1835.

Bogard D. D. and Johnson P. (1983) Martian gases in an Antarctic meteorite. *Science* **221**, 651–654.

Brearley A. J. (1998) Microstructures of feldspathic glass in ALH 84001 and evidence for post carbonate formation shock melting. *Lunar Planet. Sci. XXIX*. Lunar Planet. Inst., Houston. #1452 (abstr.).

Brenan J. (1994) Kinetics of fluorine, chlorine and hydroxyl exchange in fluorapatite. *Chem. Geol.* **110**, 195–210.

Brenan J. M. (1993) Partitioning of fluorine and chlorine between apatite and aqueous fluids at high pressure and temperature. *Earth Planet. Sci. Lett.* **117**, 251–263.

Carr M. H. (1986) Mars: A water rich planet? *Icarus* **56**, 187–216.

Carr M. H. (1996) *Water on Mars*. Oxford University Press, Oxford.

Deloule E., Albarede F., and Sheppard S. M. F. (1991) Hydrogen isotope heterogeneities in the mantle from ion probe analysis of amphiboles from ultramafic rocks. *Earth Planet. Sci. Lett.* **105**, 543–553.

Dera P., Prewitt C. T., Boctor N. Z., and Hemley R. J. (2002) Characterization of a high-pressure phase of silica from the Martian meteorite Shergotty. *Am. Mineral.* **87**, 1018–1023.

Donahue T. M. (1995) Evolution of water reservoirs on Mars from D/H ratios in the atmosphere and crust. *Nature* **374**, 432–434.

Dreibus G. and Wänke H. (1987) Volatiles on Earth and Mars: A comparison. *Icarus.* **71**, 225–240.

Dubrovinsky L. S., Saxena S. K., Lazor P., Ahuja R., Eriksson O., Wills J. M., and Johansson B. (1997) Experimental and theoretical identification of a new high pressure phase of silica. *Nature* **388**, 362–365.

Dubrovinsky L. S., Dubrovinskaia N. A., Saxena S. K., Tutti F., Rekhi S., Le Bihan T., Shen G., and Hu J. (2001) Pressure-induced transformations of cristobalite. *Chem. Phys. Lett.* **333**, 264–270.

Eberhardt P., Reber M., Krankowsky D., and Hedges R. R. (1995) The D/H and $^{18}O/^{16}O$ ratios in water from comet Halley. *Astron. Astrophys.* **302**, 301–316.

Eiler J. M., Kitchen N., Leshin L. A., and Strausberg M. (2002) Hosts of hydrogen in Alan Hills 84001: Evidence for hydrous martian salts in the oldest martian meteorite? *Meteoritics Planet. Sci.* **37**, 395–406.

Garrison D. H. and Bogard D. D. (1998) Isotopic compositions of trapped and cosmogenic noble gases in several Martian meteorites. *Meteoritics Planet. Sci.* **33**, 721–736.

Gillet P., Barrat J. A., Deloule E., Wadhwa M., Jambon A., Sautter V., Devouard B., Neuville D., Benzerara K., and Lesourd M. (2002) Aqueous alteration in the Northwest Africa 817 (NWA 817) Martian meteorite. *Earth Planet. Sci. Lett.* **203**, 431–444.

Grady M. M., Wright I. P., and Pillinger C. T. (1998) A nitrogen and argon stable isotope study of Allan Hills 84001: Implications for the evolution of the Martian atmosphere. *Meteoritics Planet. Sci.* **33**, 795–802.

Greenwood J. P. and McSween H. Y. Jr. (2001) Petrogenesis of Allan Hills 84001: constraints from impact melted feldspathic and silica glasses. *Meteoritics Planet. Sci.* **36**, 43–62.

Hauri E. H., Wang J., Dixon J. E., King P. L., Mandeville C., and Newman S. (2002) SIMS investigations of volatiles in silicate glasses, 1: Calibration, matrix effects and comparison with FTIR. *Chem. Geol.* **183**, 99–114.

Head J. W. III, Hiesinger H., Ivanov M. A., Kreslavsky M. A., Pratt S., and Thomson B. J. (1999) Possible ancient oceans on Mars: Evidence from Mars orbiter laser altimeter data. *Science* **286**, 2134–2137.

Hervig R. L. and Steele I. M. (1992) Oxygen isotopic analysis of Allende olivine by ion microprobe and implications for chondrule origin. *Lunar Planet. Sci. XXIII*. Lunar Planet. Inst., Houston., 525–526(abstr.).

Hunten D. M., Pepin R. O., and Walker J. C. G. (1987) Mass fractionation in hydrodynamic escape. *Icarus* **69**, 532–549.

Jakosky B. M. (1990) Mars atmospheric D/H: Consistent with polar volatile theory? *J. Geophys. Res.* **95**, 1475–1480.

Jakosky B. M. and Jones J. H. (1997) The history of Martian volatiles. *Rev. Geophys.* **35**, 1–16.

Jull A. J. T., Eastoe C. J., Xue S., and Herzog G. F. (1995) Isotopic composition of carbonates in the SNC meteorites Allan Hills 84001 and Nakhla. *Meteoritics* **30**, 311–318.

Jull A. J. T., Courtney C., Jeffrey D. A., and Beck J. W. (1998) Isotopic evidence for a terrestrial source of organic compounds found in Martian meteorites Allan Hills 84001 and Elephant Moraine 79001. *Science* **279**, 366–369.

Koga K., Hauri E. H., Hirschmann M. and Bell D. (2003) Hydrogen analysis by SIMS and FTIR: Comparison and calibration for nominally anhydrous minerals. *Geochem. Geophys. Geosyst.* **4,** doi: 10.1029/2002GC000378.

Lange M. A., Lambert P., and Ahrens T. J. (1985) Shock effects on hydrous minerals and implications for carbonaceous meteorites. *Geochim. Cosmochim. Acta* **49**, 1715–1726.

Leshin L. A. (2000) Insights into martian water reservoirs from analyses of the martian meteorite QUE94201. *Geophys. Res. Lett.* **27**, 2017–2020.

Leshin L. A., Epstein S., and Stolper E. M. (1996) Hydrogen isotope geochemistry of SNC meteorites. *Geochim. Cosmochim. Acta* **60**, 2635–2650.

Marti K., Kim J. S., Thakur A. N., McCoy T., and Keil K. (1995) Signature of the martian atmosphere in the glass of the Zagami meteorite. *Science* **267**, 1981–1984.

Mathew K. J. and Marti K. (2001) Early evolution of Martian volatiles: Nitrogen and noble gas components in ALH84001 and Chassigny. *J. Geophys. Res.* **106**, 1401–1422.

McCoy T., Taylor G. J., and Keil K. (1992) Zagami: Product of a two stage magmatic history. *Geochim. Cosmochim. Acta* **56**, 3571–3582.

McSween H. Y. Jr. and Jarosewich E. (1983) Petrogenesis of Elephant Moraine A79001 meteorite: Multiple pulses on the shergottite parent body. *Geochim. Cosmochim. Acta* **47**, 1501–1503.

McSween H. Y., Jr. and Treiman A. H. (1998) Martian meteorites. In *Planetary materials* (ed. J. J. Papike) pp. 6–01–6–53. Mineral. Soc. Am., Washington.

McSween H. Y. Jr., Taylor L. A., and Stolper E. (1979) Allan Hills 77005—A new meteorite type found in Antarctica. *Science* **204**, 1201–1203.

Mikouchi T., Miyamoto M., and McKay G. A. (2001) Mineralogy and petrology of the Dar al Gani 476 martian meteorite: Implications for its cooling history and relationship to other shergottites. *Meteoritics Planet. Sci.* **36**, 531–548.

Mittlefehldt D. W. (1994) ALH84001, a cummulate orthopyroxenite member of the Martian meteorite clan. *Meteoritics* **29**, 214–221.

Mittlefehldt D. W. and Linstrom M. M. (1999) Petrology and geochemistry of Martian meteorites EETA79001 and ALHA 77005. *Lunar Planet. Sci. XXX*. Lunar Planet. Inst., Houston. #1817 (abstr.).

Mittlefehldt D. W., Lindstrom D. J., Lindstrom M. M. and Martinez R. H. (1997) Lithology A in EETA 79001—Product of impact melting on Mars. *Lunar Planet. Sci. XXVIII*. Lunar Planet. Inst., Houston. 961–962(abstr.).

Mittlefehldt D. W., Lindstrom D. J., Lindstrom M. M., and Martinez R. H. (1999) An impact-melt origin for lithology A of Martian meteorite Elephant Moraine A79001. *Meteoritics Planet. Sci.* **34**, 357–368.

Mumma M. J. (1997) Organic volatiles in comets. In *From Stardust to Planetesimals* (eds. Y. J. Pendleton and A. G. G. M. Tielens), pp. 387–396. Astonomical Society of the Pacific, San Francisco.

Nadeau S. L., Epstein S., Stolper E. (1999) Hydrogen and carbon abundances and isotopic ratios in apatite from alkaline intrusive complexes, with a focus on carbonatites. *Geochim. Cosmochim. Acta* **63,** 1837–1852.

Newman S., Epstein S., and Stolper E. (1988) Water, carbon dioxide, and hydrogen isotopes in glasses from ca. 1340 A.D. eruption of the Mono craters, California: Constraints on degassing phenomena and initial volatile content. *J. Volcanology Geothermal Res.* **35**, 75–96.

Osinski G. R. and Spray J. G. (2001) Impact-generated carbonate melts: evidence from the Haughton structure, Canada. *Earth Planet. Sci. Lett.* **194**, 17–29.

Ott U. (1988) Noble gases in SNC meteorites: Shergotty, Nakhla, Chassigny. *Geochim. Cosmochim. Acta* **52**, 1937–1948.

Owen T., Maillard J. P., de Bergh C., and Lutz B. L. (1988) Deuterium on Mars: The abundance of HDO and the value of D/H. *Science* **240**, 1767–1769.

Pepin R. O. (1991) On the origin and early evolution of terrestrial planet atmospheres and meteoritic volatiles. *Icarus* **92**, 2–79.

Pepin R. O. (1994) Evolution of the Martian atmosphere. *Icarus* **111**, 289–304.

Romanek C. S., Grady M. M., Wright I. P., Mittlefehldt D. W., Socki R. A., Pillinger C. T., and Gibson E. K. Jr. (1994) Record of fluid-rock interactions on Mars from the meteorite ALH84001. *Nature* **372**, 655–657.

Santos R. V. and Clayton R. N. (1995) Variations in oxygen and carbon isotopes in carbonatites: a study of Brazilian alkaline complexes. *Geochim. Cosmochim. Acta* **59**, 1339–1352.

Schaal R. B. and Hörz F. (1977) Shock metamorphism of lunar and terrestrial basalts. *Proc. 8th Lunar Planet. Sci. Conf.* 1697–1729.

Scott E. R. D. (1999) Origin of carbonate-magnetite-sulfide assemblages in Martian meteorite ALH84001. *J. Geophys. Res.* **104**, 3803–3813.

Sharp T. G. and El Goresy A. (1999) A post stishovite SiO_2 polymorph in the meteorite Shergotty. Implications for impact events. *Science* **284**, 1511–1513.

Skinner H. C., Kittelberger J. S., and Beebe R. A. (1975) Thermal stability in synthetic hydroxyapatites. *J. Phys. Chem.* **79**, 2017–2019.

Steele I. M. and Smith J. V. (1982) Petrology and mineralogy of two basalts and olivine-pyroxene-spinel fractments in achondrite EETA 79001. *J. Geophys. Res.* **87**, A373–A384.

Stöffler D., Ostertag R., Jammes C., Pfannschmidt G., Sengupta P. R., Simon S. B., Papike J. J., and Beauchamp R. H. (1986) Shock metamorphism and petrography of the Shergotty achondrite. *Geochim. Cosmochim. Acta* **50**, 889–913.

Stöffler D., Keil K., and Scott E. R. D. (1991) Shock metamorphism of ordinary chondrites. *Geochim. Cosmochim. Acta* **55**, 3845–3867.

Stolper E. and McSween H. Y. Jr. (1979) Petrology and origin of the Shergottite meteorites. *Geochim. Cosmochim. Acta* **43**, 1475–1498.

Sugiura N. and Hoshino H. (2000) Hydrogen isotopic compositions in Allan Hills 84001 and the evolution of the martian atmosphere. *Meteoritics Planet. Sci.* **35**, 373–380.

Swindle T. D. (1995) How many Martian noble gas reservoirs have we sampled? *Volatiles in the Earth and Solar System* **341**, AIP.175–185.

Treiman A. H. (1995) A petrologic history of martian meteorite ALH84001: Two shocks and an ancient age. *Meteoritics.* **30**, 294–302.

Treiman A. H. (1998) The history of Allan Hills 84001 revised: Multiple shock events. *Meteoritics Planet. Sci.* **33**, 753–764.

Treiman A. H. and Romanek C. S. (1998) Bulk and stable isotopic compositions of carbonate minerals in Martian meteorite Allan Hills 84001: No proof of high temperature origin. *Meteoritics Planet. Sci.* **33**, 737–742.

Treiman A. H. and Sutton S. R. (1992) Petrogenesis of the Zagami meteorite: inferences from synchrotron x-ray (SXRF) microprobe and electron microprobe analysis. *Geochim. Cosmochim. Acta* **50**, 1071–1091.

Treiman A. H., McKay G. A., Bogard D. D., Mittlefehldt D. W., Wang M.-S., Keller L. P., Lipschutz M. E., Lindstrom M. M., and Garrison D. H. (1994) Comparison of the LEW88516 and ALHA77005 martian meteorites: Similar but distinct. *Meteoritics* **29**, 582–592.

Tyburczy J. A., Frisch B., and Ahrens T. J. (1986) Shock induced volatile loss from a carbonaceous chondrite: Implications for planetary accretion. *Earth Planet. Sci. Lett.* **80**, 201–207.

Tyburczy J. A., Krishnamurthy R. V., Epstein S., and Ahrens T. J. (1990) Impact induced devolatilization and hydrogen isotope fractionation of serpentine: Implications for planetary accretion. *Earth Planet. Sci. Lett.* **98**, 245–261.

Tyburczy J. A., Xu X., Ahrens T. J., and Epstein S. (2001) Shock-induced devolatilization and isotopic fractionation of H and C from Murchison meteorite: some implications for planetary accretion. *Earth Planet. Sci. Lett.* **192**, 23–30.

Valley J. W., Eiler J. M., Graham C. M., Gibson E. K., Romanek C. S., and Stolper E. M. (1997) Low-temperature carbonate concretions in the Martian meteorite ALH84001: Evidence from stable isotopes and mineralogy. *Science* **275**, 1633–1638.

Wadhwa M. and Crozaz G. (1998) The igneous crystallization history of an ancient Martian meteorite from trace element microdistributions. *Meteoritics Planet. Sci.* **33**, 685–692.

Wadhwa M., McSween H. Y. Jr., and Crozaz G. (1994) Petrogenesis of the shergottite meteorites inferred from minor and trace element microdistributions. *Geochim. Cosmochim. Acta* **58**, 4213–4229.

Wadhwa M., Lentz R. C. F., McSween H. Y. Jr., and Crozaz G. (2001) A petrologic and trace element study of Dar al Gani 476 and Dar al Gani 489: Twin meteorites with affinities to basaltic and lherzolitic shergottites. *Meteoritics Planet. Sci.* **36**, 195–208.

Warren P. H. (1998) Petrologic evidence for low-temperature, possibly flood-evaporitic origin of carbonates in the ALH84001 meteorite. *J. Geophys. Res.* **103**, 16759–16773.

Wasson J. T. and Kallemeyn G. W. (1988) Composition of chondrites. *Phil. Trans. Roy. Soc. London* **A325**, 535–544.

Watson L. A., Hutcheon I. D., Epstein S., and Stolper E. M. (1994) Water on Mars: Clues from deuterium/hydrogen and water contents of hydrous phases in SNC meteorites. *Science* **265**, 86–90.

Yung Y. L., Wen J., Pinto J. P., Allen M., Pierce K. K., and Paulsen S. (1988) HDO in the Martian atmosphere: Implications for the abundance of crustal water. *Icarus* **76**, 146–159.

Zahnle K. J. and Kasting J. F. (1986) Mass fractionation during transonic escape and implications for loss of water from Mars and Venus. *Icarus* **68**, 462–480.

Zahnle K. J., Kasting J. F., and Pollack J. B. (1990) Mass fractionation of noble gases in diffusion-limited hydrodynamic escape. *Icarus* **84**, 502–527.

Zinner E. and Crozaz G. (1986) Ion probe determination of the abundances of all the rare earth elements in single mineral grains. In *Secondary Ion Mass Spectrometry (SIMS V)* (eds. A. Benninghoven, R. J. Colton, D. S. Simons, and H. W. Werner), pp. 444–446. Springer-Verlag, New York.

Zipfel J., Scherer P., Spettle B., Dreibus G., and Schultz L. (2000) Petrology and chemistry of the new shergottite Dar al Gani 476. *Meteoritics Planet. Sci.* **35**, 95–106.

Appendix

POTENTIAL IMPLICATIONS FOR MARTIAN WATER BUDGETS OF THE ALH 84001 GLASS H ISOTOPIC COMPOSITIONS.

If the maximum H isotopic composition of the glasses in ALH 84001 is that of the atmosphere 3.9 Gyr ago, it would imply either that Mars was enriched in deuterium when it formed, or that by this time the exchangeable reservoir had lost most of its hydrogen to space. Of the likely sources of planetary water, comets are the most enriched in deuterium ($\delta D \approx 1000$ ‰) (Eberhardt et al., 1995; Mumma, 1997), but not by enough to explain the glass compositions. Hydrogen loss appears to be the explanation. Here we briefly explore the potential implications that the glass data have for the evolution of water on Mars. As elsewhere, water abundances are expressed in terms of the depth to which the water would cover the surface of Mars.

The two main mechanisms responsible for loss of hydrogen from Mars are hydrodynamic and Jeans escape (Carr, 1996). Hydrodynamic escape will have dominated in the first 100–500 Myr of Mars's history (Pepin, 1991, 1994; Jakosky and Jones, 1997). It is the best explanation for the elemental and isotopic abundances of xenon in Mars's atmosphere, but the mechanism requires huge fluxes and fluences of hydrogen (Zahnle and Kasting, 1986; Hunten et al., 1987; Zahnle et al., 1990; Pepin, 1991). The heavy carbon isotopic composition of the ALH 84001 carbonate ($\delta^{13}C = 40-46$ ‰: Romanek et al., 1994; Jull et al., 1995; Valley et al., 1997) is also qualitatively consistent with early atmospheric loss (Pepin, 1994). The models of Pepin (1991) have hydrodynamic escape occurring over the first 50–200 Myr and water losses equivalent to ~100 km covering the surface of Mars. Estimates of the amount of water accreted by Mars during formation are equivalent to ~150 km of water (Dreibus and Wänke, 1987). Thus, almost the entire initial water inventory of Mars may have been consumed by hydrodynamic escape.

Assuming a terrestrial primordial hydrogen isotopic composition, Rayleigh fractionation behavior and a hydrogen isotopic fractionation factor of $f = 0.8-0.9$ for hydrodynamic escape (Zahnle et al., 1990), the most fractionated glass composition reported ($\delta D \approx 2100$ ‰; Sugiura and Hoshino, 2000) requires that only 0.35–0.001% of the hydrogen in the exchangeable reservoir remained by 3.9 Gyr. This means that of the estimated initial 150 km of water, only between 525 m and 2 m was left by 3.9 Gyr. This is broadly consistent with water abundances equivalent to 40–400 m and 100 m needed to produce the post-Noachian (<4.3–3.5 Gyr) outflow channels (Carr, 1986) and ocean (Head et al., 1999), respectively. The post-Noachian outflow channels and ocean require that a significant fraction of the water remaining (100–400 m) was in the upper crust/exchangeable reservoir. Thus if correct, these estimates will have important implications for the water budget of the Martian mantle (≤150 ppm at 3.9 Gyr) and the conditions required to initiate melting. Also note that unless Mars accreted much more than 150 km of water, the initial D/H ratio of Mars must have been close to or greater than that of the Earth (1.6×10^{-4}), rather than nearer the initial solar value (1.6×10^{-5}). Otherwise, the amount of hydrogen loss via hydrodynamic escape required to produce the glass δD compositions would leave less water than is needed to produce the post-Noachian outflow channels and ocean.

Once hydrodynamic escape had effectively ceased, Jeans escape ($f = 0.32$; (Yung et al., 1988) would have been the dominant hydrogen loss mechanisms. Assuming no input from other sources, to evolve from $\delta D \approx 2100$ ‰ to the present day atmospheric value of $\delta D = 4200$ ‰ requires the loss of ~53% of the remaining water in the exchangeable reservoir. Using the present day hydrogen loss rate and the δD of minerals in the Zagami meteorite, Donahue (1995) estimated the amount of water in the exchangeable reservoir at 4.5 Gyr to be equivalent to 5.6–280 m of water covering the surface of Mars. Using the same approach, but also allowing that the time averaged hydrogen loss rate may have been 20× higher (Jakosky, 1990) than assumed by Donahue, the glass data suggest water abundances equivalent to 8–166 m at 3.9 Gyr. Again this is broadly consistent with the amount of water (equivalent to 100–400 m) needed to produce the post-Noachian outflow channels and ocean. Indeed, it would be problematic if the water responsible for these surface features was not part of the exchangeable reservoir, at least during this period in Martian history.